

---

Electronic Thesis and Dissertation Repository

---

June 2017

# Daily Hydrogen Sulfide Treatment Enables Early Recovery of Renal Function and Mitigates Renal Injury Following the Relief of Prolonged Urinary Obstruction

Shouzhe Lin, *The University of Western Ontario*

Supervisor: Dr. Alp Sener, *The University of Western Ontario*

A thesis submitted in partial fulfillment of the requirements for the Master of Science degree in Microbiology and Immunology

© Shouzhe Lin 2017

Follow this and additional works at: <https://ir.lib.uwo.ca/etd>



Part of the [Translational Medical Research Commons](#)

---

## Recommended Citation

Lin, Shouzhe, "Daily Hydrogen Sulfide Treatment Enables Early Recovery of Renal Function and Mitigates Renal Injury Following the Relief of Prolonged Urinary Obstruction" (2017). *Electronic Thesis and Dissertation Repository*. 4605.

<https://ir.lib.uwo.ca/etd/4605>

This Dissertation/Thesis is brought to you for free and open access by Scholarship@Western. It has been accepted for inclusion in Electronic Thesis and Dissertation Repository by an authorized administrator of Scholarship@Western. For more information, please contact [wlsadmin@uwo.ca](mailto:wlsadmin@uwo.ca).

## Abstract

Prolonged urinary obstruction can lead to renal dysfunction and irreversible injury. The recovery of renal function following decompression is heavily dependent on the degree of renal injury. This suggests that treatments aimed at mitigating renal injury could improve the recovery of renal function following decompression. Previous studies have shown that hydrogen sulfide (H<sub>2</sub>S), an endogenous gasotransmitter, can reduce the histopathological markers of renal injury following unilateral ureteral obstruction (UUO). However, the effects of H<sub>2</sub>S on renal function following decompression is unknown. Using the UUO and reimplantation (UUO-R) model, we demonstrate that H<sub>2</sub>S accelerates the recovery of renal function following decompression and mitigates renal injury. *In vitro*, H<sub>2</sub>S attenuates the transforming growth factor beta 1-mediated epithelial-mesenchymal transition pathway by increasing the expression of inhibitory Smad7 and angiotensin II type 2 receptor. These data suggest that H<sub>2</sub>S could potentially be a novel therapeutic strategy to improve patient outcomes in urinary obstruction.

## Keywords

Unilateral ureteral obstruction; hydrogen sulfide; renal function; renal injury; EMT; TGF-β1

## Acknowledgments

This project would have not been possible without those who supported me along the way. I would like to thank the past and present members of the Sener lab, Dr. Manujendra Saha, Dr. Hong Hai, Jas Grewal, Megan Verrydt, Jennifer Leigh, Justin Chan, Max Zhang, and Smriti Juriasingani, for their continuous support. To Dr. Ian Lobb, thank you for your endless patience and guidance. Your mentorship and friendship mean a lot to me. To the talented microsurgeons of Matthew Mailing Center for Translational Transplant Studies, Drs. Dameng Lian and Jifu Jiang, thank you for your patience and expertise, for this project would not have been possible without your assistance. I would also like to thank Dr. Weihua Liu and Dr. Aaron Haig for their help in processing and analyzing our samples. Many thanks to my advisory committee, Drs. Hassan Razvi and Jeremy Burton, your guidance and input were instrumental to the growth of this project. Finally, I would like to thank my incredible supervisor, Dr. Alp Sener. You have taught me to be a better scientist and individual. Thank you for your endless enthusiasm, support, encouragement, and mentorship.

# Table of Contents

Abstract.....	i
Acknowledgments.....	ii
Table of Contents.....	iii
List of Figures.....	vi
Chapter 1.....	1
1 Introduction.....	1
1.1 Obstructive uropathy: background and etiology.....	1
1.2 Pathogenesis of obstructive uropathy.....	1
1.2.1 Hemodynamics and functional changes.....	2
1.2.2 Tubular injury and cell death.....	3
1.2.3 Tissue inflammation.....	4
1.2.4 Tubulointerstitial fibrosis.....	4
1.3 Recovery upon the relief of ureteral obstruction.....	6
1.4 Animal models of obstructive uropathy.....	6
1.5 Pharmacological interventions in obstruction.....	7
1.6 Endogenous gasotransmitters and their potential roles in the treatment of obstruction.....	8
1.6.1 Nitric oxide.....	9
1.6.2 Carbon monoxide.....	9
1.6.3 Hydrogen sulfide.....	10
1.7 Conclusions and future therapeutic implications.....	13
1.8 Research aims and hypotheses.....	14
Chapter 2.....	16
2 Materials and Methods.....	16

2.1	Animal description and care .....	16
2.2	Optimizing and establishing a reversible unilateral ureteral obstruction model... 16	
2.2.1	Optimizing the duration of urinary obstruction .....	16
2.2.2	Optimizing the surgical protocol of a reversible UUO model.....	17
2.2.3	Unilateral ureteral obstruction and reimplantation (UUO-R) model and post-operative care .....	17
2.3	Histopathological evaluation .....	20
2.3.1	Histology.....	20
2.3.2	Immunohistochemistry .....	20
2.3.3	Immunofluorescence.....	20
2.3.4	Image analysis.....	20
2.4	Measurement of urinary H <sub>2</sub> S levels .....	21
2.5	Cell culture and treatment.....	21
2.6	Western blot.....	22
2.7	Statistical Analysis.....	22
	Chapter 3.....	23
3	Results.....	23
3.1	Daily administration of GYY4137 increases H <sub>2</sub> S levels in urine.....	23
3.2	Supplemental H <sub>2</sub> S slightly improves post-obstructive survival rates following prolonged UUO.....	24
3.3	H <sub>2</sub> S treatment improves renal function during UUO and enables early recovery of renal function post-obstruction .....	25
3.4	Exogenous H <sub>2</sub> S helps to regulate sodium excretion shortly after relief of obstruction.....	28
3.5	Administration of H <sub>2</sub> S moderately modulates proteinuria.....	30
3.6	Supplemental H <sub>2</sub> S reduces cortical loss following relief of urinary obstruction..	32
3.7	H <sub>2</sub> S mitigates renal apoptosis following relief of long-term UUO.....	34
3.8	H <sub>2</sub> S mitigates neutrophil infiltration.....	36

3.9 Supplemental H <sub>2</sub> S mediates macrophage infiltration .....	38
3.10 Exogenous H <sub>2</sub> S ameliorates renal fibrosis following relief of prolonged UUO...	42
3.11 H <sub>2</sub> S attenuates the TGF-β1-mediated EMT pathway <i>in vitro</i> .....	44
Chapter 4.....	50
4 Discussion .....	50
4.1 Summary of study.....	50
4.2 H <sub>2</sub> S from GYY4137 localizes to the kidney.....	51
4.3 H <sub>2</sub> S accelerates the recovery of renal function.....	52
4.4 Daily administration of H <sub>2</sub> S mitigates renal injury.....	54
4.5 H <sub>2</sub> S mitigates the histopathological markers of renal injury following the relief of urinary obstruction.....	56
4.6 Elucidating the potential mechanisms of action .....	60
4.7 Conclusions and future implications.....	64
References.....	66
Curriculum Vitae .....	74

## List of Figures

Figure 1. Unilateral ureteral obstruction and reimplantation model in rats.....	19
Figure 2. Urinary H <sub>2</sub> S levels increase upon daily IP injection with GYY4137.....	23
Figure 3. H <sub>2</sub> S treatment slightly improves survival of animals post-obstruction.....	24
Figure 4. Daily administration of H <sub>2</sub> S accelerates the recovery of renal function following the relief of UUO.....	27
Figure 5. Daily administration of H <sub>2</sub> S markedly decreases the fractional excretion of sodium at POD 17.....	29
Figure 6. Supplemental H <sub>2</sub> S moderately reduces proteinuria.....	31
Figure 7. H <sub>2</sub> S modulates cortical loss associated with UUO following decompression .....	33
Figure 8. Daily treatment with H <sub>2</sub> S mitigates apoptosis following relief of urinary obstruction.....	35
Figure 9. Supplemental H <sub>2</sub> S reduces neutrophil infiltration following long-term UUO and relief of obstruction.....	37
Figure 10. GYY4137 mediates macrophage infiltration in urinary obstruction.....	41
Figure 11. H <sub>2</sub> S treatment mitigates renal fibrosis following prolonged UUO and decompression.....	43
Figure 12. H <sub>2</sub> S mitigates the TGF- $\beta$ 1-induced epithelial-mesenchymal transition in NRK52E cells .....	49
Figure 13. Proposed mechanism of action of H <sub>2</sub> S in TGF- $\beta$ 1-mediated EMT pathway .....	63

## Chapter 1

### 1 Introduction

#### 1.1 Obstructive uropathy: background and etiology

Obstructive uropathy is characterized by abnormalities in the urinary tract that result in the blockage of urine flow. The prevalence and etiology of obstructive uropathy vary with age. Obstructions in children are typically caused by congenital defects that arise during embryonic development, resulting in anatomical abnormalities that obstruct the urinary tract. Congenital obstructive uropathy is one of the leading causes of end stage renal disease (ESRD) in children and accounts for 16.5% of all pediatric renal transplantations in North America (Roth et al. 2002). In the young and middle-aged adult, urinary obstructions are typically caused to obstructive calculi (kidney stones). Studies estimate that approximately 10-15% of Americans will develop obstructive stones in their lifetime, with 40% risk of recurrence at 5 years and 75% at 20 years (Spernat & Kourambas 2011). In the elderly, urinary tract obstructions are more common in males and are typically caused by benign prostatic hyperplasia or prostate cancer (Klahr 2000). Ureteral obstructions can be unilateral or bilateral, and can be classified based on degree (complete or partial obstruction) and duration (acute and chronic). In this review, we will focus on the outcomes, pathophysiology, and potential therapies for obstructive uropathy.

#### 1.2 Pathogenesis of obstructive uropathy

Urinary tract obstruction is one of the many causes of acute kidney injury (AKI) and chronic kidney disease (CKD). A possible treatment for AKI is dialysis, a process which can take days to weeks. While the mortality rate of AKI is approximately 50%, death from CKD-related injury or the need for dialysis and renal transplantation is generally the ultimate outcome of CKD (Ucero et al. 2014). AKI and CKD share similar pathogenesis, including cellular injury, cell death and inflammation. In addition, tubulointerstitial



fibrosis is often observed in CKD and can also be detected in severe cases of AKI. Chronic UUU can lead to irreversible renal injury and dysfunction (Ucero et al. 2014).

### 1.2.1 Hemodynamics and functional changes

Upon complete unilateral obstruction, an initial increase in renal blood flow into the obstructed kidney is observed. This is a result of prostaglandin and prostacyclin production due to medullary compression. After a few hours, and as the obstruction persists, renal blood flow decreases. This is caused by increased vascular resistance and production of vasoconstrictors such as angiotensin II (Ang II) and thromboxane A<sub>2</sub>. Together, these events lead to the decrease in glomerular filtration rate (GFR). Correspondingly, an initial increase in intratubular pressure is observed. While this rise is observed in the first few hours, intratubular pressure decreases to pre-obstructive values within the first 24 hours. The decline in pressure is caused by decreased GFR, decreased sodium reabsorption, and increased removal of tubular fluid through lymphatic drainage. Collectively, these actions decrease renal fluid volume (Klahr 2000).

Obstruction can also cause functional changes in tubular cells. Initially, there is an increase in sodium reabsorption in the tubules to mediate renal fluid volume. However, as the obstruction persists, sodium wasting occurs due to tubular injury and defects in the sodium/potassium ATPase enzymes. This disrupts the lumen potential necessary for hydrogen and potassium excretion, and the retention of hydrogen results in renal tubular acidosis. Furthermore, this prevents the distal nephrons from concentrating urine, which contributes to diuresis and inability to acidify urine upon relief of obstruction (Klahr 2000).

In chronic obstructive uropathy, the reduction of renal blood flow is maintained, which places the kidney in a state of ischemia. Consequently, reactive oxygen species (ROS)

that are harmful to renal tubular cells are generated, resulting in tubular injury and activation of the renin-angiotensin system (RAS). The subsequent increase in Ang II recruits inflammatory cells to the site of injury, ultimately leading to cell death and the release of transforming growth factor beta 1 (TGF- $\beta$ 1) (Klahr 2000).

### 1.2.2 Tubular injury and cell death

Tubular cell death occurs via apoptosis or necrosis and is a result of the mechanical and oxidative stress associated with ureteral obstruction. Apoptosis (cell suicide) is the main form of cell death observed in urinary obstruction and CKD (Ucero et al. 2014), and is characterized by chromosome condensation and cellular blebbing. This form of cell death is regulated by increased expression of intracellular lethal molecules and downregulation of pro-survival mediators. A large variety of factors associated with obstruction, such as ischemia, hypoxia, Ang II, ROS, tumour necrosis factor  $\alpha$  (TNF- $\alpha$ ), and mechanical stretching, can lead to mitochondrial destabilization and release of cytochrome C. This ultimately stimulates the caspase-mediated apoptotic pathway and contributes to tubular cell loss (Truong et al. 2001). These apoptotic cells are subsequently removed by infiltrating macrophages and neighbouring native cells (Truong et al. 2001).

Necrosis, on the other hand, is characterized by loss of cell membrane integrity and uncontrolled release of intracellular contents. Lethal stimuli released due to tissue injury and oxidative stress cause necrotic cell death, which results in the release of damage-associated molecular patterns (DAMPs) such as high-mobility group box 1. The release of DAMPs activates toll-like receptors, which recruits leukocytes to the site of injury and subsequently initiates tissue inflammation (Lech & Anders 2013). Though prominent in the early stages of pathogenesis and inflammation, necrosis is not frequently observed in chronic renal injury (Ucero et al. 2014).

### 1.2.3 Tissue inflammation

Interstitial inflammation is an early response to obstructive uropathy, and is characterized by infiltration of leukocytes that are attracted to the cytokines, chemokines, and membrane adhesion molecules released by injured renal parenchymal and endothelial cells. Interstitial leukocyte population increases from 12 hours to up to 14 days post-obstruction and consists predominantly of macrophages (Ucero et al. 2014). Macrophages can be classically activated (M1) to produce cytokines and chemokines that induce inflammation, tubular apoptosis, and fibrosis, or alternatively activated (M2) to attenuate inflammation. Classically activated macrophages generate ROS and TNF- $\alpha$ , which ultimately exacerbate the death of renal epithelial cells (Kluth et al. 2004). Additionally, interleukin (IL)-1 $\beta$  production can be observed. Together with TNF- $\alpha$ , IL-1 $\beta$  targets nuclear factor- $\kappa$ B (NF- $\kappa$ B) to increase the production of pro-inflammatory mediators such as monocyte chemoattractant protein-1 (MCP-1) and IL-1 $\beta$  (Sakurai et al. 1996), resulting in an amplified inflammatory response. M2 macrophages, on the other hand, appear in the later stages of inflammation. They play a critical role in the uptake of apoptotic cells and are known to suppress immune responses and induce tissue remodeling (Kluth et al. 2004). These macrophages release IL-4, IL-13, IL-10 and TGF- $\beta$ 1 to reduce tissue inflammation and induce tissue repair. Importantly, TGF- $\beta$ 1 plays a crucial role in the induction of fibrosis, which leads to tissue scarring and loss of function (Lech & Anders 2013).

### 1.2.4 Tubulointerstitial fibrosis

As chronicity of inflammation associated with obstructive uropathy persists, fibrosis characteristic of CKD can eventually be observed. This is characterized by activation of fibroblasts that deposit extracellular matrix (ECM) components, such as fibronectin, collagen type I and III into the interstitial space (Eddy et al. 2012). These fibroblasts can be a result of resident fibroblasts proliferation or derived from tubular epithelial cells undergoing epithelial-mesenchymal transition (EMT) (Samarakoon et al. 2012). TGF- $\beta$ 1 is a profibrotic cytokine released during inflammation and plays a critical role in

initiating the EMT response. Upon stimulation with TGF- $\beta$ 1, Smad 2 and Smad 3 protein are phosphorylated to induce fibrosis, while Smad 7, an inhibitor of the fibrotic pathway, is degraded via ubiquitination. Under these circumstances, renal epithelial cells lose their adhesions to neighbouring cells and basement membrane, increase expression of mesenchymal proteins such as vimentin, decrease expression of epithelial proteins such as E-cadherin, and migrate into the interstitium (Ucero et al. 2014; Chevalier 2006). Propagation of tubulointerstitial fibrosis is commonly observed in CKD and can lead to irreversible renal injury and loss of renal function (Iwano & Neilson 2004).

Due to its ability to stimulate TGF- $\beta$ 1, Ang II is also a key mediator in the initiation of renal fibrosis. Previous studies have demonstrated that administration of enalapril, an angiotensin-converting enzyme (ACE) inhibitor, leads to decreased production of TGF- $\beta$ 1 mRNA (Kaneto et al. 1993), and treatment with losartan, an angiotensin AT1 receptor inhibitor, attenuated the progression of renal fibrosis (Manucha et al. 2004). Additionally, the synthesis of active TGF- $\beta$ 1 requires the conversion of latent preproTGF- $\beta$ 1 to the biologically active form of TGF- $\beta$ 1, a process that is promoted by RAS (Gibbons et al. 1992). Taken together, these studies suggest that Ang II plays a critical role in the initiation of renal fibrosis through stimulation of TGF- $\beta$ 1 production. The increase in TGF- $\beta$ 1 leads to the induction of EMT in renal epithelial cells and ultimately results in tubulointerstitial fibrosis characteristic of CKD (Xu et al. 2009).

In addition, Ang II contributes to fibrosis by indirectly increasing the proliferation of renal fibroblasts. Ang II produced as a result of ureteral obstruction causes vasoconstriction and therefore local ischemia and hypoxia. Tubular cells subsequently undergo atrophy and cell death due to restricted blood flow, reduced nutrients, and depleted oxygen supply. The remaining cells undergo hypermetabolism, resulting in increased oxygen consumption and ultimately, perpetuation and exacerbation of hypoxia in the interstitium. This causes fibroblasts to proliferate and induce ECM production by epithelial cells (Iwano & Neilson 2004). Furthermore, Ang II stimulates TNF- $\alpha$

production, which increases the formation of superoxide anions and perpetuates inflammation, thereby indirectly exacerbating the progression of fibrosis (Iwano & Neilson 2004).

### 1.3 Recovery upon the relief of ureteral obstruction

While surgical removal of obstruction removes the source of injury, recovery of renal function is dependent on the duration of the obstruction and renal function may not return back to pre-obstructive state (Vaughan JR. & Gillenwater 1971). Studies demonstrate that relief of obstruction was not able to recover the 40% loss of nephrons and did not improve tubular proliferation (Chevalier et al. 1999). In addition, relief of obstruction was not able to fully return TGF- $\beta$ 1 and vimentin expression to normal levels, suggesting that tubular injury continues to persist (Chevalier et al. 1999). Similarly, Chaabane *et al.* observed a 40% reduction in GFR and a 50% reduction of glomerulotubular integrity after a 30-day recovery following a 7-day obstruction (Chaabane et al. 2013). Furthermore, albuminuria was also observed, implicating residual glomerular injury (Chaabane et al. 2013). Therefore, while relief of obstruction attenuates renal injury, complete reversal is unlikely and residual injury in the post-obstructed kidney may lead to renal dysfunction in later life. Thus, prevention of renal injury during obstruction may be a potential treatment option to improve post-obstructive renal function (Chevalier et al. 1999).

### 1.4 Animal models of obstructive uropathy

One of the most widely used experimental models of renal injury and urinary obstruction is the unilateral ureteral obstruction (UUO) model. Male animals are typically used in this experimental model, as female sex organs increase the technical difficulty of the procedure. After placing the animal under general anesthesia, a midline incision is made in the abdomen and the left ureter is found. Two sutures, one proximal and one distal to the kidney, are made in the ureter to permanently ligate the ureter. This procedure inflicts

renal injury upon the obstructed kidney while allowing the contralateral kidney to compensate for the unilateral loss of function (Ucero et al. 2014). There are several advantages of this model: it is a relatively simple procedure, it does not involve the use of an exogenous toxin, and it does not create a uremic environment (Chevalier et al. 2009). Additionally, this model can be used to explore both acute and chronic renal injury, as the initial insult can result in AKI and persistence of obstruction can produce histological indices of CKD, particularly fibrosis, after a few weeks (Ucero et al. 2014). While renal injury in the UUO model can be histologically evaluated, functional changes of the obstructed kidney cannot be determined as the contralateral kidney compensates for the loss of renal function. Tapmeier *et al.* developed the unilateral ureteral obstruction and reimplantation (UUO-R) model, in which the obstructed ureter is reimplanted into the bladder, thus emulating relief of obstruction. The contralateral kidney is subsequently removed, which causes the animal to depend solely on the previously obstructed kidney and allows for both histological and functional evaluation of the obstructed kidney (Tapmeier et al. 2008).

## 1.5 Pharmacological interventions in obstruction

To complement surgical relief of obstruction, pharmacological treatments may be used to prevent the recurrence of stones, treat existing stones, or manage symptoms associated with obstruction. Diuretics, such as thiazide diuretics and indapamide, can decrease calcium excretion and therefore reduce the risk of calcium stone formation. While beneficial, these drugs may cause hypocitriuria, hypokalemia, hyponatremia, dizziness, weakness, and gastrointestinal upset (York et al. 2015). Potassium citrate and sodium citrate are two common urinary alkalinizers used to prevent crystallization, however, like diuretics, they may also cause gastrointestinal distress. Additionally, a common side effect of potassium-containing therapeutics is hyperkalemia, which can potentially be dangerous in patients with renal failure (York et al. 2015). To treat uric acid stones, xanthine oxidase inhibitors are often used as they decrease urinary acid excretion, however they are often associated with hepatotoxicity, skin rashes, and gastrointestinal distress (York et al. 2015). Due to poor intestinal or renal tubular transport of cystine,

high urinary cystine levels may cause cystine stone formation. As such, Tiopronin and D-penicillamine are typically used to form disulfides to decrease cystine excretion and reduce the risk of cystine stone formation (York et al. 2015). Furthermore, severe flank pain is a common symptom among patients with urinary obstruction. As a result, acetaminophen, cyclooxygenase-inhibitors, non-steroidal anti-inflammatory drugs (NSAID) and opioids are typically prescribed to mediate pain. However, these drugs can have mild to severe side effects, including gastrointestinal distress, hepatotoxicity, respiratory depression, and addiction (York et al. 2015). Several pharmacological interventions are available to induce the expulsion of urinary stones. For instance, alpha-blockers may improve the expulsion of urinary stones by inducing ureter relaxation, however, these drugs may cause nausea and nasal congestion (York et al. 2015). While effective, these drugs are not able to mitigate the accumulation of renal injury during obstruction. If prolonged, obstruction can cause irreversible renal injury and lead to permanent loss of renal function (Kerr JR 1956). Furthermore, studies have shown that relief of obstruction can only mitigate, but not reverse, renal injury (Wu et al. 2012). Therefore, preemptive therapies administered during the course of obstruction may help improve renal function following the relief of obstruction.

## 1.6 Endogenous gasotransmitters and their potential roles in the treatment of obstruction

Recent evidence suggests that gasotransmitters can exhibit anti-inflammatory and anti-oxidant effects in various models of tissue injury (Wang 2002). Gasotransmitters are small, endogenously produced gaseous molecules that have specific cellular and molecular targets, can freely permeate membranes, and have physiological functions (Qian & Matson 2016). Currently, nitric oxide (NO), carbon monoxide (CO), and hydrogen sulfide (H<sub>2</sub>S) are identified as gasotransmitters.

### 1.6.1 Nitric oxide

NO is produced endogenously by nitric oxide synthases (NOSs), a family of enzymes including inducible NOS (iNOS), neuronal NOS (nNOS) and endothelial NOS (eNOS), from L-arginine. Classically, NO acts by activating soluble guanylate cyclase (sGC) to increase the production of 3',5'-cyclic guanosine monophosphate (cGMP), ultimately leading to the activation of protein kinases and mediate various physiological responses (Qian & Matson 2016). For instance, in the circulatory system, NO can induce smooth muscle cell relaxation to cause vasodilation, thus making it an excellent therapeutic option for hypertension and related cardiovascular diseases (Qian & Matson 2016). In inflammatory processes, NO can act as a 'double-edged sword' depending on its concentration. Pro-inflammatory cytokines can cause an upregulation of iNOS in macrophages and neutrophils and lead to an excessive production of NO (Sharma et al. 2007). Consequently, more phagocytes are recruited to the site of inflammation and through positive feedback, generate supra-physiological concentrations of NO, which can lead to sepsis (Kumar et al. 2017). However, at low concentrations, NO plays an anti-inflammatory role by reducing the expression of endothelial cell adhesion molecules and thus mitigate inflammation by inhibiting leukocyte adhesion to the endothelium (Lefer & Lefer 1999). Furthermore, studies have shown that treatment with L-arginine ameliorates renal fibrosis, apoptosis, and inflammation following UUO, which suggests that NO may serve as a potential therapy against damages associated with urinary obstruction (Sun et al. 2012).

### 1.6.2 Carbon monoxide

Heme oxygenases (HO), both inducible and constitutive, convert heme into iron, biliverdin, and CO. Interestingly, the production of NO and CO are closely related: CO can bind to NOS to increase NO production and NO can activate inducible HO to stimulate CO production. Like NO, CO can also diffuse through cell membranes and bind to sGC to increase cGMP production and cause smooth muscle relaxation (Gibbons & Farrugia 2004). Though toxic at high concentrations, CO can be therapeutic at low doses.



For instance, like NO, CO also exhibits anti-inflammatory effects due to its ability to mitigate the production of pro-inflammatory cytokines and increase the production of anti-inflammatory mediators (Motterlini & Foresti 2013). In renal ischemia reperfusion injury (IRI), CO has been shown to decrease oxidative stress, tubular apoptosis and inflammation (Abe T, Fujino M, Yazawa K, Imamura R, Hatayama N, Kakuta Y, Tsutahara K, Okumi M, Ichimaru N, Kaimori JY, Isaka Y, Seki K, Takahara S, Li X-K 2017). Studies by Wang et al. have demonstrated that in low-dose treatment with CO in UUO leads to decreased renal fibrosis. CO can mitigate ECM deposition *in vivo* and attenuate the TGF- $\beta$ 1-mediated fibrosis pathway *in vitro* (Wang et al. 2008). Through controlled inhalation or administration of CO-releasing molecules (CORM), CO can exhibit therapeutic effects in various models of tissue injury, as demonstrated in the lung, liver, intestine, and kidney (Bauer & Pannen 2009; Wallace et al. 2015; Qian & Matson 2016).

### 1.6.3 Hydrogen sulfide

Along with NO and CO, H<sub>2</sub>S was recently identified as the third gasotransmitter. Using L-cysteine, H<sub>2</sub>S is endogenously produced by cystathionine  $\beta$ -synthase (CBS), cystathionine  $\gamma$ -lyase (CSE) and 3-mercaptopyruvate sulfurtransferase (3-MST); these enzymes are expressed in majority of human cell types, producing H<sub>2</sub>S in the nanomolar to micromolar range (Whiteman et al. 2011). By acting on K<sub>ATP</sub> channels, H<sub>2</sub>S exerts physiological effects on the cardiovascular system by mediating smooth muscle cell relaxation and vasodilation (Wang 2002). Additionally, H<sub>2</sub>S can mediate metabolism, scavenge ROS, mitigate apoptosis and reduce inflammation (Wang 2002; Lobb et al. 2014). Due to its broad variety of function, disruption of H<sub>2</sub>S production has been implicated in diseases such as hypertension, cancer, CKD and diabetes (Whiteman et al. 2011). In the kidney, CSE, CBS and 3-MST are primarily found in the proximal tubules (Yamamoto et al. 2013). These enzymes play a major role in regulating renal hemodynamics by altering blood flow, GFR, and urine excretion due to its vasodilatory properties (Xia et al. 2006). In addition, H<sub>2</sub>S may play a role in regulating renin-angiotensin system (RAS) via modulation of cAMP and ROS production (Xue et al.

2013). Due to its multifaceted effects on renal physiology, dysregulation of H<sub>2</sub>S production has been implicated in chronic kidney disease and other renal pathologies (Lobb et al. 2014).

### 1.6.3.1 Hydrogen sulfide in ureteral obstruction

In ureteral obstruction, H<sub>2</sub>S has been shown to mediate tubulointerstitial fibrosis, oxidative stress, and inflammation. Tubulointerstitial fibrosis has been associated with decreased expression of CBS and CSE, and therefore decreased H<sub>2</sub>S concentration (Jung et al. 2013). Interestingly, Jung *et al.* has demonstrated that exogenous treatment with sodium hydrogen sulfide (NaHS, a H<sub>2</sub>S producer) can mediate the decrease in CBS and CSE expression (Jung et al. 2013). Furthermore, after seven days of treatment, NaHS reduced fibrosis and mitigated the increase in TGF- $\beta$ 1, Smad3, and NF- $\kappa$ B expression, suggesting that the H<sub>2</sub>S production pathway may be a potential target for mediating fibrosis associated with ureteral obstruction (Jung et al. 2013).

The induction of fibrosis is exacerbated by oxidative stress, as ROS have been reported to increase the expression Ang II and TGF- $\beta$ 1 (Song et al. 2015). Therefore, mitigating ROS production may potentially be a way to alleviate tubulointerstitial fibrosis. A study by Jiang *et al.* demonstrated that exogenous treatment with NaHS significantly alleviated oxidative stress associated with UUO after 10 days of treatment (Jiang et al. 2014). When compared to control, UUO animals treated with NaHS demonstrated decreased expression of malondialdehyde (MDA, a marker for increase lipid peroxidation associated with ROS accumulation) and increased expression of superoxide dismutase (SOD, a free radical-scavenging enzyme) (Jiang et al. 2014). Correspondingly, NaHS significantly attenuated fibrosis associated with UUO (Jiang et al. 2014). Therefore, due to its anti-oxidant properties, H<sub>2</sub>S may potentially reduce UUO-induced renal injury.

The anti-inflammatory properties of H<sub>2</sub>S are well-established (Szabó 2007). As previously discussed, inflammation plays a crucial role in the development and progression of fibrosis. A study by Song *et al.* demonstrated that, in a rat model of UUO, H<sub>2</sub>S treatment mitigated inflammation and attenuated fibrosis (Song et al. 2014). After treating UUO animals with NaHS for 7 days, decreased infiltration of macrophages and reduced expression of IL-1 $\beta$ , TNF- $\alpha$  and MCP-1 mRNA were observed when compared to control animals (Song et al. 2014). Similarly to Jiang *et al.*, Song *et al.* also observed that NaHS can alleviate fibrotic injury by attenuating TGF- $\beta$ 1 expression and fibroblast proliferation (Song et al. 2014).

Collectively, these studies suggest that the ant-fibrotic effects of H<sub>2</sub>S may in part be mediated by its anti-oxidant and anti-inflammatory properties. Taken together, these findings suggest that exogenous H<sub>2</sub>S may be a potential therapy against renal injury associated with UUO.

### 1.6.3.2 GYY4137, a slow-releasing hydrogen sulfide donor

The use of H<sub>2</sub>S in literature have largely been limited to sulfide salts such as NaHS. These molecules release supra-physiological amounts of H<sub>2</sub>S instantaneously in solution, therefore unlikely to emulate the slow and sustained release of H<sub>2</sub>S in biological systems. GYY4137 is a novel water-soluble H<sub>2</sub>S donor that releases H<sub>2</sub>S over a sustained period of time (from hours to days) (Li et al. 2008). Studies have shown that exposing vascular smooth muscle cells to low concentrations of GYY4137 leads to sustained vasorelaxation, as opposed to the transient effects of NaHS (Li et al. 2008). To evaluate the effects of GYY4137 on inflammation, Li *et al.* evoked inflammation in mice by administering lipopolysaccharide. Upon treatment with GYY4137, they observed reduced macrophage infiltration, along with decreased expression of TNF- $\alpha$  and IL-1 $\beta$ , confirming that GYY4137 retains the anti-inflammatory properties of H<sub>2</sub>S (Li et al. 2013). Additionally, Lin et al. has recently demonstrated the anti-inflammatory and anti-

fibrotic of GYY4137 in a rat model of chronic UUO. Mirroring the downregulation of EMT markers in renal tissue, administration of GYY4137 also attenuated the progression of EMT *in vitro* (Lin et al. 2016). Taken together, these studies conclude that GYY4137 is a slow-releasing H<sub>2</sub>S donor molecule with anti-inflammatory, anti-apoptotic, anti-oxidant, and anti-fibrotic properties and can exhibit protective effects in various models of tissue injury.

### 1.6.3.3 Development of clinically viable hydrogen sulfide-releasing therapeutics

Due to the promise that H<sub>2</sub>S holds, there has been a surge in research and development of clinically viable H<sub>2</sub>S-donors, such as garlic-derived compounds including allyl disulfide, and more recently, H<sub>2</sub>S-releasing drugs, such as sodium polysulthionate (SG-1002), Zofenopril and ATB-346 (Wallace et al. 2017). SG-1002 has been shown to restore plasma H<sub>2</sub>S and NO levels in patients with congenital heart failure, and has recently been approved for Phase 2 clinical trials (Wallace et al. 2017). Zofenopril is an ACE inhibitor prodrug that metabolizes to zofenoprilat, a sulfhydryl-containing metabolite. It exhibits cardioprotective and vasculoprotective properties, and due to its sulfhydryl moiety, also exhibits anti-oxidant effects (Wallace et al. 2017). Though NSAIDs are commonly used to mediate pain and inflammation, they often carry the risk of gastrointestinal distress, bleeding, and ulceration. Antibe Therapeutics recently developed ATB-346, a naproxen-based drug linked to an H<sub>2</sub>S-donor, with the aim of using the gastroprotective effects of H<sub>2</sub>S to help mediate the side effects associated with NSAIDs. ATB-346 has recently successfully completed Phase 2 clinical trials in patients with osteoarthritis (Wallace et al. 2017).

## 1.7 Conclusions and future therapeutic implications

Prolonged ureteral obstruction can lead to accumulation of renal damage, ultimately resulting in loss of renal function. While surgical relief of obstruction removes the source

of insult, renal function and renal injury may not be fully reversed, and this residual injury can lead to renal dysfunction in later life. H<sub>2</sub>S possesses several protective properties and has been shown to mitigate the accumulation of renal injury in chronic UUO. This suggests that, in the future, H<sub>2</sub>S-based therapeutics may potentially be used to improve post-obstructive renal function and clinical outcomes. Though still in the early stages of development, H<sub>2</sub>S-releasing drugs show considerable promise. If administered throughout the duration of UUO, H<sub>2</sub>S-releasing drugs may be a potential solution to attenuate renal damage and improve renal function following relief of urinary obstruction.

## 1.8 Research aims and hypotheses

While various groups have explored the effects of H<sub>2</sub>S on ureteral obstruction using the UUO model (Song et al. 2014; Jiang et al. 2013; Lin et al. 2016), a limitation of the UUO model lies in the fact that renal injury can only be determined histopathologically. However, the aim of a therapeutic intervention is to improve renal function. Thus, we propose to use the UUO-R model (Tapmeier et al. 2008) to evaluate the effects of H<sub>2</sub>S treatment on renal function following the relief of urinary obstruction. We will administer H<sub>2</sub>S donor GYY4137 during obstruction, as well as during obstruction and following decompression. We will then evaluate the functional response of the kidney following the relief of obstruction. Additionally, we intend to determine the mechanisms behind the anti-fibrotic properties of GYY4137 through *in vitro* assays.

**Aim 1:** To investigate the effects of GYY4137 on renal function following the relief of ureteral obstruction.

**Hypothesis:** GYY4137 treatment will mitigate renal damage and improve renal function.

**Aim 2:** To determine the mechanism by which GYY4137 mitigates fibrosis by employing an *in vitro* model of EMT using a rat kidney epithelial cell line (NRK52E).

**Hypothesis:** GYY4137 will attenuate fibrosis by moderating the TGF- $\beta$ 1-mediated EMT pathway.

## Chapter 2

### 2 Materials and Methods

#### 2.1 Animal description and care

Adult male Lewis rats (250-300g; *Charles River Laboratories International Ltd.*) were maintained in the Animal Care and Veterinary Services facility at Western University. Animals were managed in accordance with the guidelines set by Committee on Care and Use of Laboratory Animals of the Institute of Laboratory Animal Resources, National Research Council. All experiments were approved by Council on Animal Care and Animal Use Subcommittee of Western University. In accordance to the “reduce-reuse-recycle” philosophy established by the Animal Use Subcommittee, we used the fewest number of animals in our study to establish a biological and statistical significance.

#### 2.2 Optimizing and establishing a reversible unilateral ureteral obstruction model

The UUO model is a widely accepted model used to mimic urinary obstruction and study renal injury(Kaneto et al. 1993). However, renal injury can only be determined through histopathological methods, and as the contralateral kidney remains intact, the UUO model cannot provide data regarding the function of the affected kidney post-obstruction. As such, we sought to employ a reversible UUO model to evaluate renal function post-obstruction.

##### 2.2.1 Optimizing the duration of urinary obstruction

The duration of urinary obstruction was optimized such that it inflicts sufficient renal injury while allowing for functional recovery post-obstruction. Male Lewis rats underwent UUO procedure(Kaneto et al. 1993). Briefly, rats anesthetized with ketamine (30 mg/kg) and maintained under anesthesia with 1% isoflurane. The left ureter was

ligated at the ureterovesical junction, as close to the bladder as possible. Rats were sacrificed on post-operative day (POD) 3, 7, and 14 (n=2 each), and the left kidney was removed for histological analysis with terminal deoxynucleotidyl-transferase-mediated dUTP nick end labeling (TUNEL) and Masson's trichrome. A renal pathologist blind to the animals' assignment groups evaluated the slides to determine the optimal duration of ligation and ideal severity of renal injury. The optimal duration of obstruction was determined to be 14 days.

### **2.2.2 Optimizing the surgical protocol of a reversible UUO model**

A reversible UUO surgical protocol was established to allow us to evaluate post-obstructive renal function. We adapted the surgical procedure established by Chaabane et al. to a 14-day rat urinary obstruction model (Chaabane et al. 2013). Rats (n=2) were placed under general anesthesia. A catheter was placed adjacent to the left ureter, and the ureteral ligation was completed by suturing the ureter to the catheter. On POD14, the catheter was cut to release the ligation. However, the integrity of the ureter was compromised, resulting in death due to urine leakage. To prevent urine leakage, we further modified this model by inserting a stent into the ureter after relief of obstruction on POD14. However, this was not a viable model as the stent injured the lumen of the ureter and caused ureteral bleeding.

### **2.2.3 Unilateral ureteral obstruction and reimplantation (UUO-R) model and post-operative care**

The UUO-R model established by Tapmeier et al. was successfully modified to a 14-day model in rats (Tapmeier et al. 2008). Male Lewis rats were randomly divided into 4 groups: Sham (n=5), UUO-R (n=10), UUO-R + 14 day GYY4137 (n=11), and UUO-R + 30 day GYY4137 (n=5). All animals were placed under general anesthesia. Sham animals underwent midline incision and closure, while all other animals underwent UUO procedure (the left ureter was directly ligated at the ureterovesical junction). The incision



was closed and animals were placed back into their cages. From POD 1 to 14, rats in UUO-R group received daily intraperitoneal (IP) injections of phosphate buffered saline (PBS, 1 mL, vehicle), while rats in the UUO-R + 14 day GYY4137 and UUO-R + 30 day GYY4137 received daily IP injections of GYY4137 (200  $\mu$ mol/kg GYY4137 in 1 mL PBS).

On POD 14, all rats were placed under anesthesia and a midline incision was made. Sham rats underwent right nephrectomy and closure. All other rats underwent the reimplantation procedure. Briefly, the obstructed ureter was freed of surrounding adhesions and the ligature was cut such that the ureter was unobstructed and urine flowed freely through the ureter lumen. An 18-gauge needle was pushed into the left side of bladder, into the cavity, and out through the right bladder wall. Using forceps to hold the sharp end of the needle, the needle and forceps were back pushed through the bladder and out the left side of the bladder. The distal end of the unobstructed ureter was grasped with forceps and pulled into the bladder cavity and out through the right bladder wall. Using 10-0 silk sutures, 12 stitches were placed to secure the ureter to the left bladder wall. The distal end of the ureter was allowed to move back into the bladder, and the defect on the right bladder wall was closed with 10-0 silk sutures. A right nephrectomy was performed to allow animals to depend solely on the previously obstructed kidney. The midline incision was closed and the animals were returned to their cages. Rats in the UUO-R + 30 day GYY4137 continued to receive daily IP injections of GYY4137 from POD 15 to 30. On PODs 3, 7, 10, 17, 21, 24, and 30, or until sacrifice, all animals were placed in metabolic cages for 24-hour to measure water intake and urine output. In addition, 200 $\mu$ L of blood was collected from tail vein and centrifuged at 10000xg for 10 minutes to obtain serum. Serum and urine samples were analyzed at London Health Science Centre (LHSC) Core Laboratory for serum creatinine and electrolytes and urine creatinine, protein, and electrolytes. Animals were sacrificed on POD 30. As two animals in the UUO-R group were euthanized prematurely on POD 18 due to renal failure, a subset of animals were sacrificed on POD 18 (UUO-R, n=3; UUO-R + 14 day GYY4137, n=5) for

analysis. The left kidney was removed at time of sacrificed and divided sagittally, with half used for either histological or RNA and protein analysis.

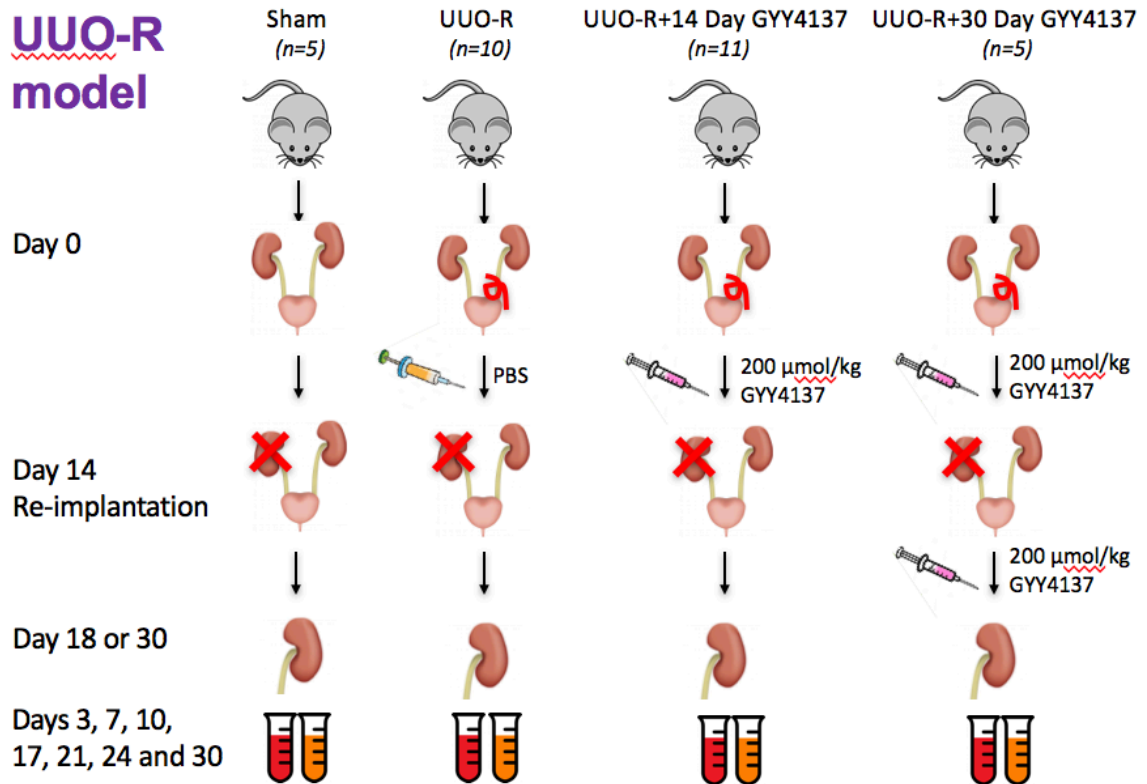


**Figure 1. Unilateral ureteral obstruction and reimplantation model in rats.**

## 2.3 Histopathological evaluation

### 2.3.1 Histology

Tissues were stored in 10% formalin, embedded in paraffin and sectioned. Subsequently, sections were stained with hematoxylin and eosin (H&E). Sections were also stained with TUNEL (*Genetex*) to quantify the number of apoptotic cells and Masson's trichrome (*Abcam*) to determine the degree of fibrosis.

### 2.3.2 Immunohistochemistry

Macrophage and neutrophil infiltration were determined via immunohistochemistry (IHC) with antibodies against CD68 (*Abcam*) and myeloperoxidase (MPO, *Abcam*), respectively. IHC sections were visualized using the Dako Envision System with secondary antibodies and DAB substrate chromogen as per manufacturer's protocol.

### 2.3.3 Immunofluorescence

Quantification of M1 and M2 macrophages was determined through immunofluorescence (IF). Slides were incubated with antibodies against CD68 and CD206 (*Abcam*), followed by AlexaFluor 405-conjugated and AlexaFluor 488-conjugated secondary antibodies, as per manufacturer's protocol.

### 2.3.4 Image analysis

Whole-slide scans of H&E sections were taken with ScanScope AT Turbo Aperio (*Leica Biosystems*) and cortical thickness was measured by a blinded renal pathologist. TUNEL, Masson's trichrome, and IHC (CD68 and MPO) sections were imaged using Nikon Eclipse 90i light microscope at 10x magnification at 5 random areas. *Image J* software (*National Institute of Health*) was used to quantify the number of positive cells or positively stained areas of fibrosis. IF samples were viewed with FLUOVIEW X831

confocal microscope (*Olympus*) at 40x magnification. Images were acquired with FLUOVIEW FV10 ASW4.0 viewer. Number of CD68<sup>+</sup> (blue), CD206<sup>+</sup> (green), and CD68<sup>+</sup>/CD206<sup>+</sup> (cyan, overlay of blue and green) cells were quantified using *Image J* software.

## 2.4 Measurement of urinary H<sub>2</sub>S levels

MeRho-Az (Sonke et al. 2015; Hammers et al. 2015), an H<sub>2</sub>S-specific fluorescent probe, was used to determine if daily IP injection of 200 μmol/kg GYY4137 increased urinary levels of H<sub>2</sub>S. MeRho-Az was generously donated by Dr. Michael Pluth (*University of Oregon, Eugene, OR*). Male Lewis rats were divided into two groups, UUO (n=5) and UUO + GYY4137 (n=5), and all animals underwent UUO procedure as described above. From POD 1 to POD 3, rats in the UUO group received daily IP injections of PBS (1 mL) while animals in the UUO + GYY4137 group received daily IP injections of GYY4137 (200 μmol/kg GYY4137 in 1 mL PBS). At sacrifice (POD 3), 25-gauge needle was inserted into the obstructed ureter to collect urine. Immediately, 20 μM of MeRho-Az was added to urine and samples were flash frozen with liquid nitrogen and stored in -80°C. To determine the concentration of H<sub>2</sub>S in urine, a standard curve was made with sodium sulfide (Na<sub>2</sub>S•9H<sub>2</sub>O) in 20 μM of MeRho-Az. Standards and urine samples were pipetted into 96-well plates. Fluorescence intensity of samples was quantified using a fluorescent plate reader (Synergy H4 Hybrid Reader, *BioTek*) at  $\lambda_{\text{excitation}} = 476 \text{ nm}$  and  $\lambda_{\text{emission}} = 516 \text{ nm}$ .

## 2.5 Cell culture and treatment

NRK52E cells (*ATCC*) were seeded in 6 well plates at  $1.5 \times 10^5$  cells/well with Dulbecco's Modified Eagle's Medium (DMEM, *Thermo Fisher Scientific*) supplemented with 5% fetal bovine serum (FBS) and 1% penicillin and streptomycin at 37°C under 5% CO<sub>2</sub>. At 90% confluency, cells were serum starved with basic DMEM for 24 hours. Subsequently, cells were either treated with 10ng/mL TGF-β1 (*Peprotech*), 10 μM

GY4137, 50  $\mu$ M GYY4137, 10 ng/mL TGF- $\beta$ 1+10  $\mu$ M GYY4137, 10 ng/mL TGF- $\beta$ 1+50  $\mu$ M GYY4137 or untreated in serum-free DMEM for 48 hours.

## 2.6 Western blot

Protein from NRK52E cells was collected using RIPA lysis buffer (*Thermo Fisher Scientific*) as per manufacturer's protocol and quantified using NanoDrop 1000 Spectrophotometer (*Thermo Scientific*). 50  $\mu$ g of protein was separated by SDS-PAGE, transferred onto a nitrocellulose membrane and probed with antibodies against glyceraldehyde 3-phosphate dehydrogenase (GAPDH), E-cadherin, transforming growth factor beta 1 receptor 2 (TGF- $\beta$ 1R2), vimentin (*GeneTex*), cofilin and angiotensin II type 2 receptor AT2R (*Abcam*). Secondary antibodies were Horseradish peroxidase-linked anti-rabbit or anti-mouse (*GeneTex*). Proteins were detected using ImmunStar Western C (*Bio-rad Laboratories*). Chemiluminescent signals were detected using FluorChem M System (*Protein Simple*). Protein expression was quantified by densitometry using the *Image J* software and normalized to GAPDH or cofilin.

## 2.7 Statistical Analysis

Kaplan-Meier survival analysis was used to analyze survival data. Biochemical and histological data were analyzed using one-way ANOVA. All other data were analyzed using unpaired Student's t-test. All statistical analysis was performed using GraphPad Prism version 7.0. P-values < 0.05 were considered statistically different.

## Chapter 3

### 3 Results

#### 3.1 Daily administration of GYY4137 increases H<sub>2</sub>S levels in urine

To investigate if GYY4137 (200  $\mu\text{mol/kg}$ ) administered daily through IP injections released and delivered H<sub>2</sub>S to the kidneys, we used MeRho-Az, a fluorescent H<sub>2</sub>S probe, to measure urinary H<sub>2</sub>S levels. After three days of UUO, urine obtained directly from the obstructed ureter of GYY4137-treated rats had significantly higher levels of H<sub>2</sub>S ( $p < 0.05$ ) compared to UUO rats (Figure 2).

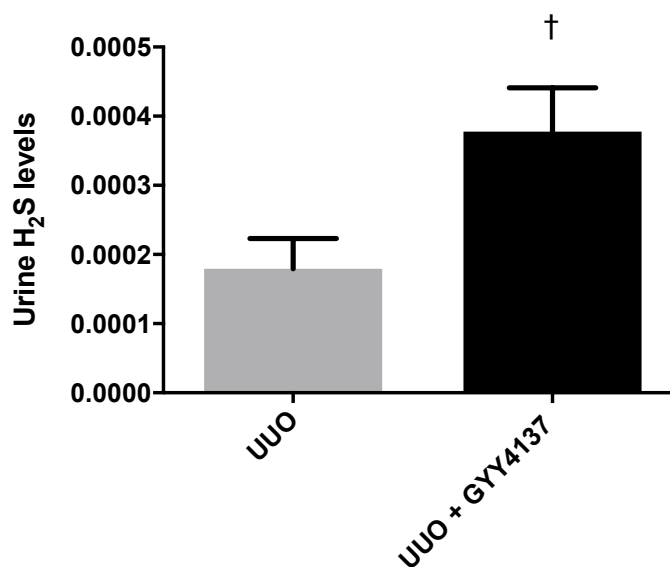


**Figure 2. Urinary H<sub>2</sub>S levels increase upon daily IP injection with GYY4137.** Urine was obtained directly from obstructed kidney in UUO (n=5, 1mL PBS IP daily) and UUO + GYY4137 (n=5, 200  $\mu\text{mol/kg}$  GYY4137 in 1 mL PBS, IP daily) rats on POD 3. 200  $\mu\text{M}$  of MeRho-Az fluorescent H<sub>2</sub>S probe was added immediately upon urine collection and samples were flash frozen in liquid nitrogen. Urinary concentration of H<sub>2</sub>S was determined based on fluorescence intensity. Values are mean  $\pm$  SEM. † $p < 0.05$  vs. UUO

### 3.2 Supplemental H<sub>2</sub>S slightly improves post-obstructive survival rates following prolonged UUU

After relief of obstruction and reimplantation, we observed a slight improvement in survival rates in GYY4137-treated groups compared to UUU-R group. While all GYY4137-treated animals survived until POD 30, two animals in the UUU-R group did not survive past POD 19 (Figure 3).

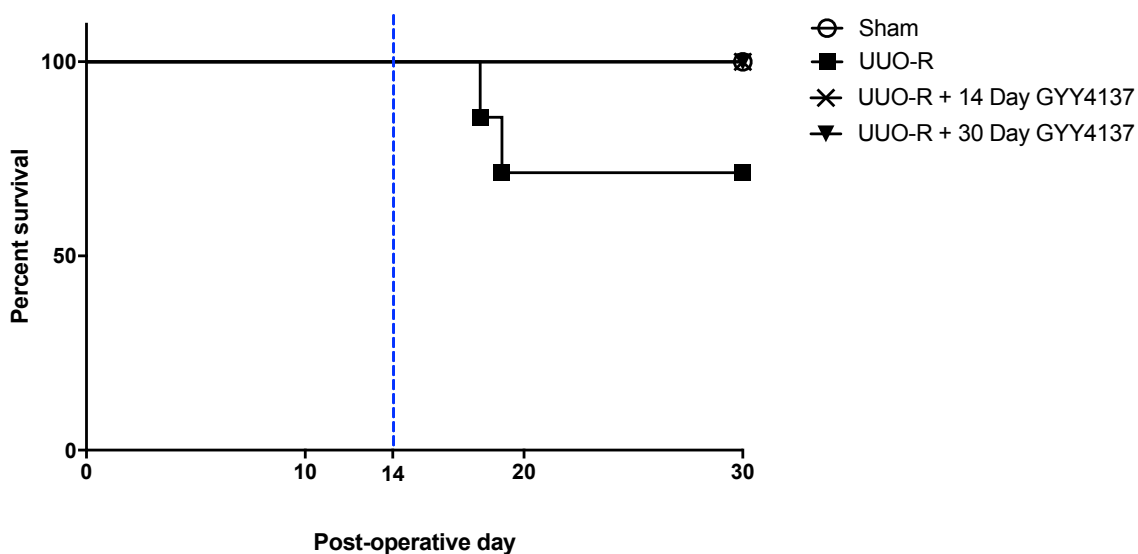


**Figure 3. H<sub>2</sub>S treatment slightly improves survival of animals post-obstruction.**

Survival rates of Sham (n=5), UUO-R (n=10, 1mL PBS IP daily), UUO-R + 14 Day GYY4137 (n=11, 200  $\mu$ mol/kg GYY4137 in 1 mL PBS, IP daily POD 1-14), UUO-R + 30 Day GYY4137 (n=5, 200  $\mu$ mol/kg GYY4137 in 1 mL PBS, IP daily POD 1-30) animals. Blue line indicates day of reimplantation surgery (day 14).

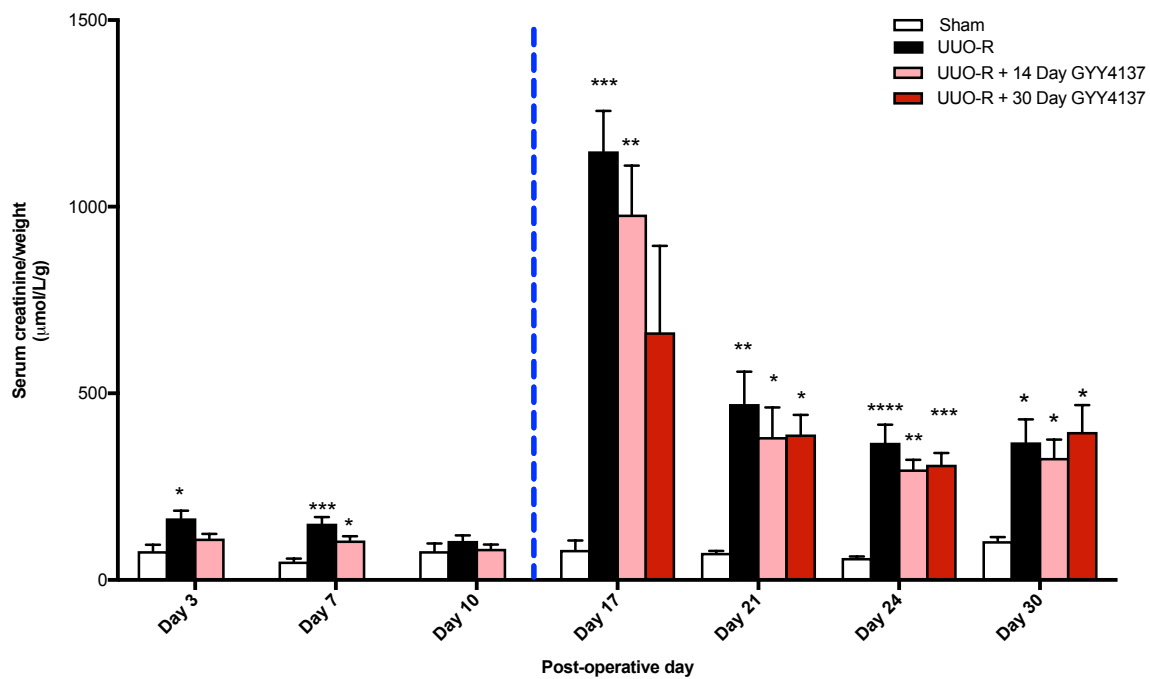
### 3.3 H<sub>2</sub>S treatment helps to improve renal function during UUO and enables earlier recovery of renal function post-obstruction

On POD 3 and 7, serum creatinine levels of UUO-R rats were significantly higher than Sham-operated rats ( $p < 0.01$ ). Serum creatinine levels of GYY4137-treated rats were also significantly higher than Sham on POD 7 ( $p < 0.05$ ). However, serum creatinine levels of GYY4137-treated animals were not higher than Sham on POD 3 and 10. All experimental groups exhibited significantly higher serum creatinine levels when compared to Sham ( $p < 0.05$ ) following decompression. Interestingly, while UUO-R, UUO-R + 14 Day GYY4137 and UUO-R + 30 Day GYY4137 groups all exhibited higher serum creatinine levels than Sham on POD 17 ( $p < 0.0001$ ,  $p < 0.01$ ,  $p < 0.05$ , respectively), continuous administration of GYY4137 upon relief of obstruction resulted in a marked reduction in serum creatinine levels when compared to UUO-R group on POD 17 (Figure 4A).

Serum cystatin C levels of all experimental groups were higher than Sham on POD 18 ( $p < 0.05$ ), however, treatment with GYY4137 markedly reduced serum cystatin C levels when compared to UUO-R animals (Figure 4B). Cystatin C levels in UUO-R, UUO-R + 14 Day GYY4137 and UUO-R + 30 Day GYY4137 animals were not different from Sham on POD 30 (Figure 4B).



A)



B)

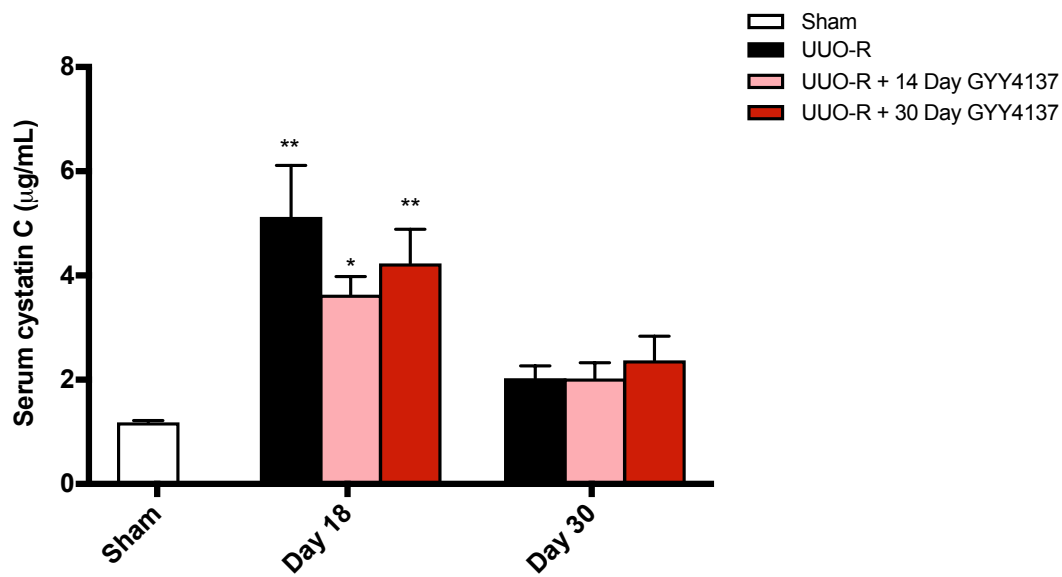


**Figure 4. Daily administration of H<sub>2</sub>S accelerates the recovery of renal function following the relief of UUO.** Serum samples were obtained on POD 3, 7 10, 17, 21, 24 and 30 from Sham (n=5), UUO-R (n=10, 1mL PBS IP daily), UUO-R + 14 Day GYY4137 (n=11, 200 μmol/kg GYY4137 in 1 mL PBS, IP daily POD 1-14), UUO-R + 30 Day GYY4137 (n=5, 200 μmol/kg GYY4137 in 1 mL PBS, IP daily POD 1-30) rats for analysis of A) creatinine levels and normalized to body weight on day of serum collection and B) cystatin C levels. Values are mean ± SEM. Blue dashed line indicates day of reimplantation. \* p<0.05, \*\*p<0.01, \*\*\* p<0.001, \*\*\*\* p<0.0001 vs Sham.

### 3.4 Exogenous H<sub>2</sub>S helps to regulate sodium excretion shortly after relief of obstruction

The fractional excretion of sodium (FENa) of UUO-R, UUO-R + 14 Day GYY4137 and UUO-R + 30 Day GYY4137 groups were drastically higher when compared to Sham on POD 17. Though not statistically different, FENa of GYY4137-treated animals was considerably lower than UUO-R animals on POD 17 (Figure 5). The FENa of UUO-R, UUO-R + 14 Day GYY4137, and UUO-R + 30 Day GYY4137 were all similar to Sham on POD 30 (Figure 5).

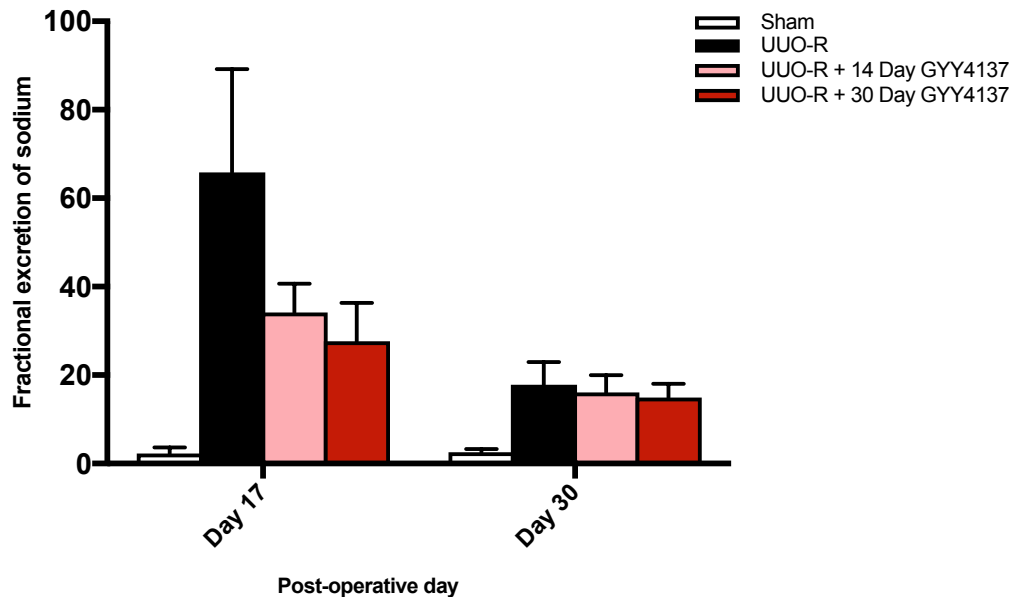


**Figure 5. Daily administration of H<sub>2</sub>S markedly decreases the fractional excretion of sodium at POD 17.** Urine and serum samples were obtained on POD 17 and 30 from Sham (n=5), UUO-R (n=10, 1mL PBS IP daily), UUO-R + 14 Day GYY4137 (n=11, 200  $\mu$ mol/kg GYY4137 in 1 mL PBS, IP daily POD 1-14), UUO-R + 30 Day GYY4137 (n=5, 200  $\mu$ mol/kg GYY4137 in 1 mL PBS, IP daily POD 1-30) rats for analysis. Values are mean  $\pm$  SEM.

### 3.5 Administration of H<sub>2</sub>S moderately modulates proteinuria

During the obstruction period, 24-hour total urine protein excretion in obstructed animals was similar to Sham-operated animals (Figure 6). Following the relief of obstruction, urinary protein levels were remarkably higher in all experimental groups when compared to Sham group. On POD 17, urine protein was significantly increased in UUO-R animals when compared to Sham on ( $p < 0.05$ ), however administration of GYY4137 following relief of obstruction led to a moderate decrease in urine protein excretion. On all other post-obstructive days, urine protein in UUO-R group was considerably higher when compared to Sham, though not statistically significant. Treatment with GYY4137 resulted in a trend towards a decrease in urine protein when compared to UUO-R group (Figure 6).

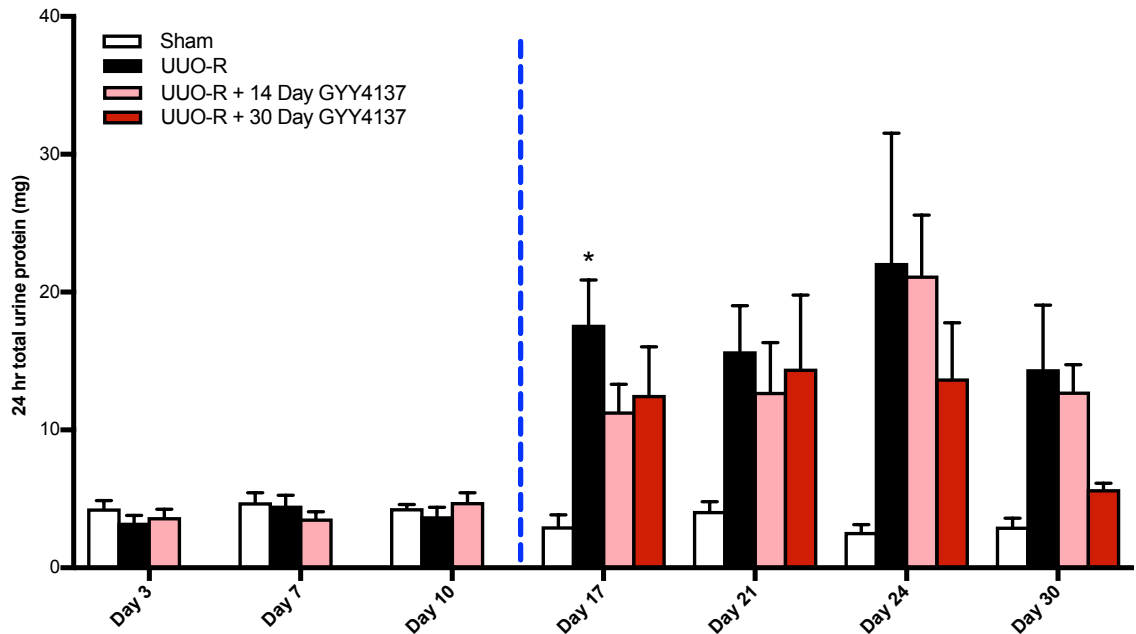
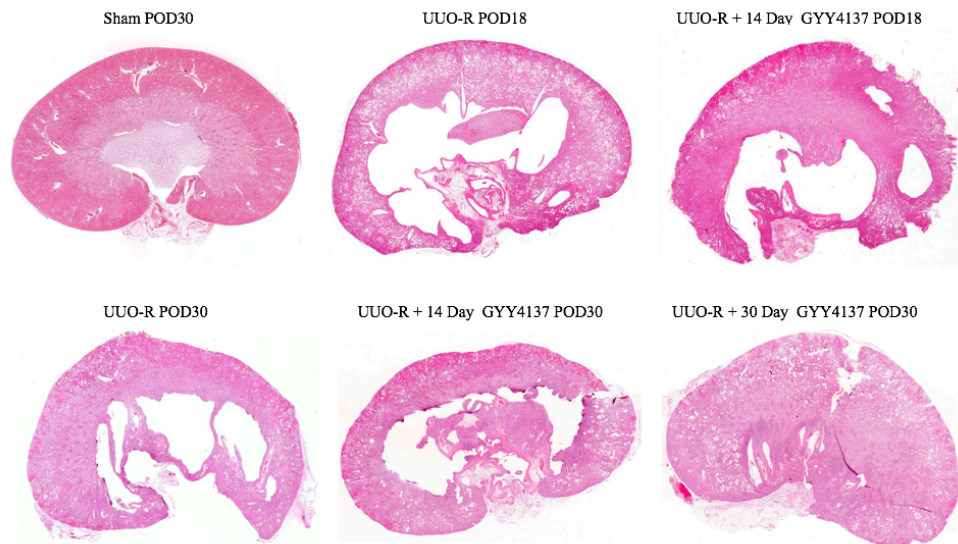


**Figure 6. Supplemental H<sub>2</sub>S moderately reduces proteinuria.** Urine samples were obtained on POD 3, 7 10, 17, 21, 24 and 30 from Sham (n=5), UUO-R (n=10, 1mL PBS IP daily), UUO-R + 14 Day GYY4137 (n=11, 200  $\mu$ mol/kg GYY4137 in 1 mL PBS, IP daily POD 1-14), UUO-R + 30 Day GYY4137 (n=5, 200  $\mu$ mol/kg GYY4137 in 1 mL PBS, IP daily POD 1-30) rats for quantification of urine protein concentration and 24 hour urine volume. 24 hour urine protein excretion was quantified. Values are mean  $\pm$  SEM. Blue dashed line represents day of reimplantation. \*p<0.05 vs. Sham

### 3.6 Supplemental H<sub>2</sub>S reduces cortical loss following relief of urinary obstruction

To evaluate the effect of GYY4137 on renal architecture following UUO-R, kidney sections were stained with H&E and cortical thickness was measured by a blinded renal pathologist (Figure 7A). On POD 18, rats in the UUO-R and UUO-R + 14 Day GYY4137 group both had significantly decreased renal cortical thickness when compared to Sham ( $p < 0.05$ ). The cortical thickness of UUO-R and UUO-R + 14 Day GYY4137 were all significantly lower on POD 30 when compared to Sham ( $p < 0.05$ ), however, 30-day treatment with GYY4137 significantly rescued cortical loss when compared to UUO-R POD 30 ( $p < 0.05$ , Figure 7B).

A)



B)

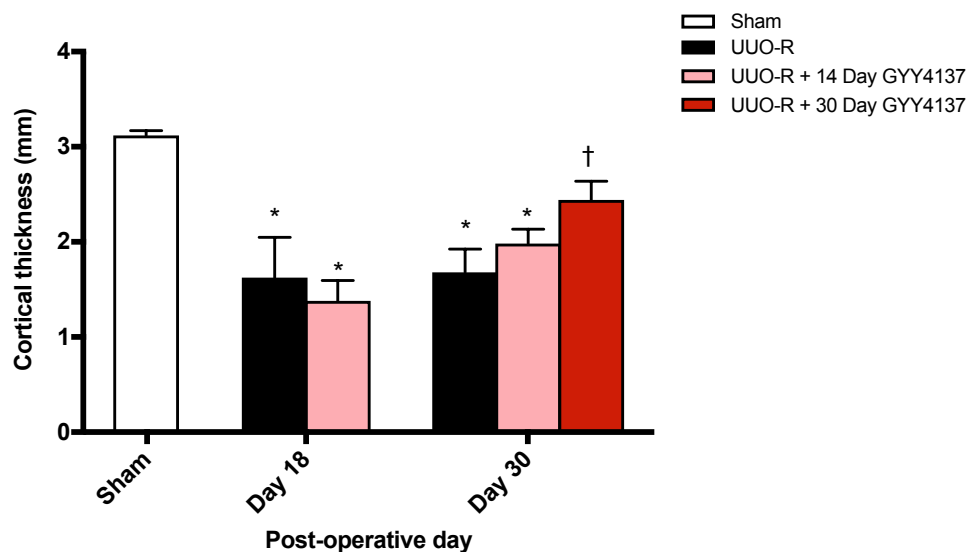


**Figure 7. H<sub>2</sub>S modulates cortical loss associated with UUO following decompression.**

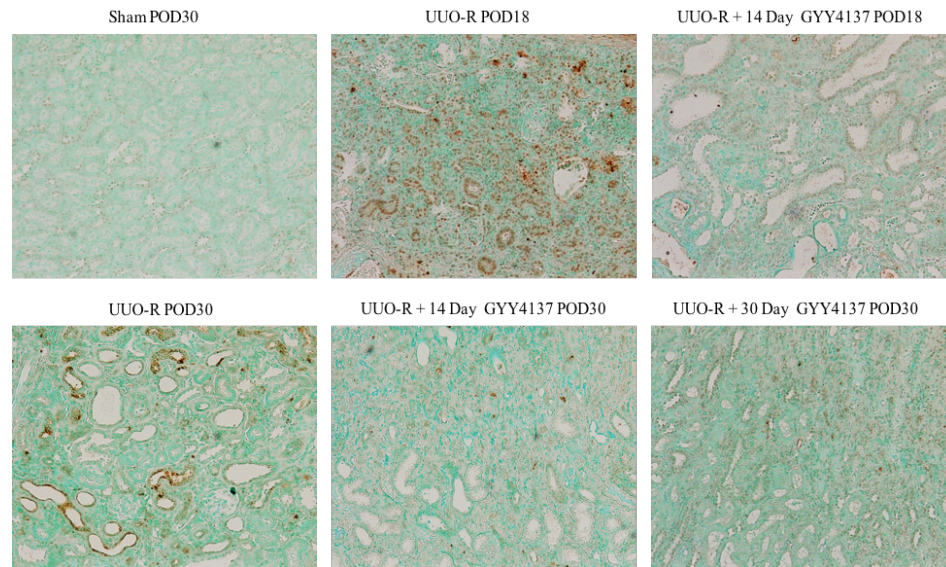
Kidney samples were obtained from Sham (n=5), UUO-R (n=10, 1mL PBS IP daily), UUO-R + 14 Day GYY4137 (n=11, 200  $\mu$ mol/kg GYY4137 in 1 mL PBS, IP daily POD 1-14), UUO-R + 30 Day GYY4137 (n=5, 200  $\mu$ mol/kg GYY4137 in 1 mL PBS, IP daily POD 1-30) rats on POD 18 and POD 30. Sections were stained with H&E. A) Representative whole-slide scans of kidney sections. B) Cortical thickness was measured by a blinded renal pathologist. Values are mean  $\pm$  SEM. \*p<0.05 vs Sham POD30, †p<0.05 vs UUO-R POD30.



### 3.7 H<sub>2</sub>S mitigates renal apoptosis following relief of long-term UUO

Tissue sections were stained with TUNEL to quantify the number of apoptotic cells (Figure 8A). When compared to Sham-operated animals, UUO-R animals had a marked increase in renal apoptosis on POD 18 and UUO-R + 14 Day GYY4137 animals exhibited significantly higher levels of apoptosis ( $p < 0.05$ ) on POD 18. The UUO-R + 14 Day GYY4137 group have a considerably lower level of apoptosis when compared to UUO-R group on POD 18, though not statistically significant. While UUO-R and UUO-R + 14 Day GYY4137 group both exhibited significantly higher levels of apoptosis when compared to Sham ( $p < 0.01$  and  $p < 0.05$ , respectively), UUO-R + 30 Day GYY4137 group had similar levels of apoptosis when compared to Sham on POD 30. Renal apoptosis associated with UUO-R was significantly ameliorated on POD 30 upon 30 days of GYY4137 treatment ( $p < 0.01$ ), and interestingly, 30-day administration of GYY4137 led to a significant decrease in apoptosis when compared to 14-day GYY4137 treatment ( $p < 0.05$ , Figure 8B).

A)



B)

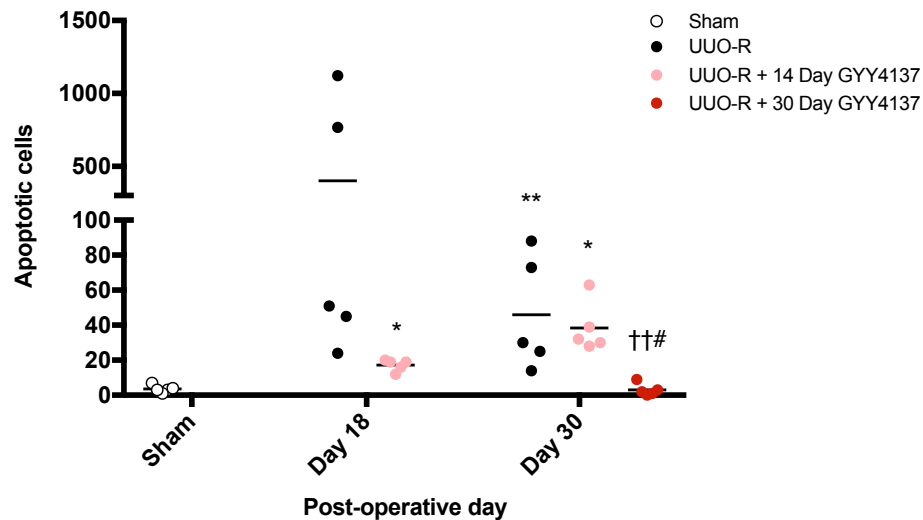
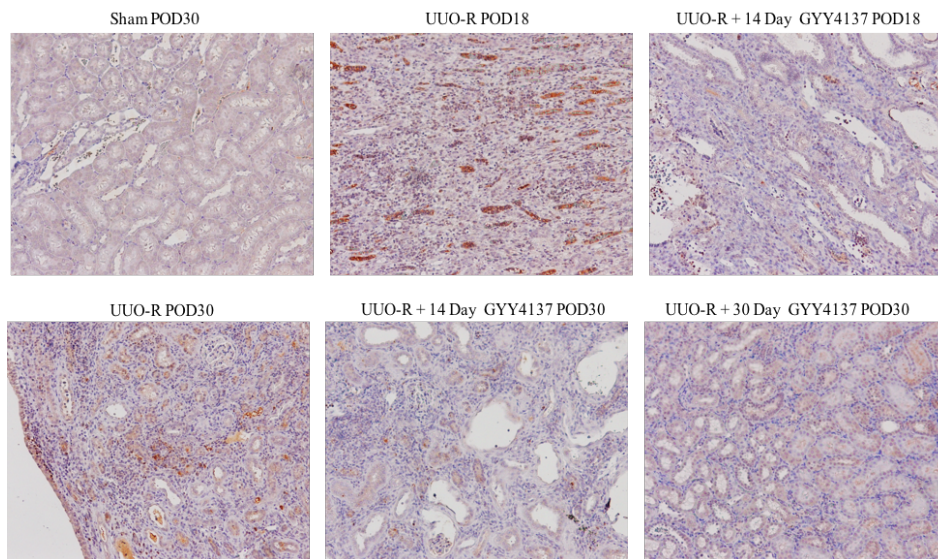


**Figure 8. Daily treatment with H<sub>2</sub>S mitigates apoptosis following relief of urinary obstruction.** Terminal deoxynucleotidyl-transferase-mediated dUTP nick end labeling (TUNEL) staining of kidneys following Sham (n=5), UUO-R (n=10, 1mL PBS IP daily), UUO-R + 14 Day GYY4137 (n=11, 200  $\mu$ mol/kg GYY4137 in 1 mL PBS, IP daily POD 1-14), UUO-R + 30 Day GYY4137 (n=5, 200  $\mu$ mol/kg GYY4137 in 1 mL PBS, IP daily POD 1-30) on POD18 and POD30. A) Representative images of sections stained with TUNEL at 10x magnification. B) Median cell count of 5 randomly acquired images at 10x magnification, quantified using ImageJ. Bar represents mean. \* p<0.05, \*\*p<0.01, vs Sham POD30, ††p<0.05 vs UUO-R POD30, #p<0.05 vs UUO-R + 14 Day GYY4137

### 3.8 H<sub>2</sub>S mitigates neutrophil infiltration

To determine the effects of GYY4137 on neutrophil infiltration, kidney sections were immunohistochemically stained with antibody against MPO (Figure 9A). On POD 18, UUO-R group exhibited significantly higher levels of neutrophil infiltration when compared to Sham ( $p < 0.05$ ), while UUO-R + 14 Day GYY4137 group did not. While it was not statistically significant, the number of neutrophils in the UUO-R + 14 Day GYY4137 group was considerably lower when compared to UUO-R group on POD 18 (Figure 9B). On POD 30, UUO-R groups exhibited significantly higher levels of neutrophil infiltration when compared to Sham ( $p < 0.05$ ). UUO-R + 14 Day GYY4137 and UUO-R + 30 Day GYY4137 groups, however, were similar to Sham on POD 30. Moreover, UUO-R + 30 Day GYY4137 animals exhibited significantly lower levels of neutrophil infiltration when compared to UUO-R ( $p < 0.05$ , Figure 9B).

A)



B)

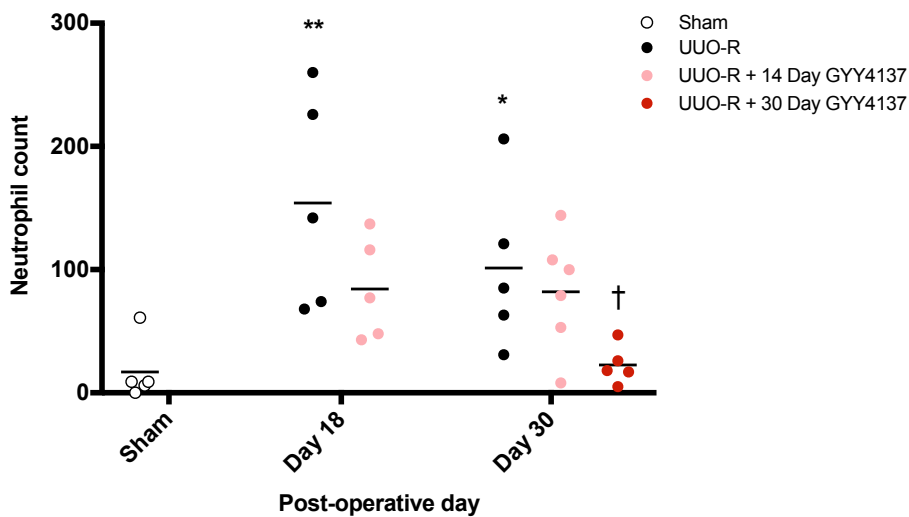
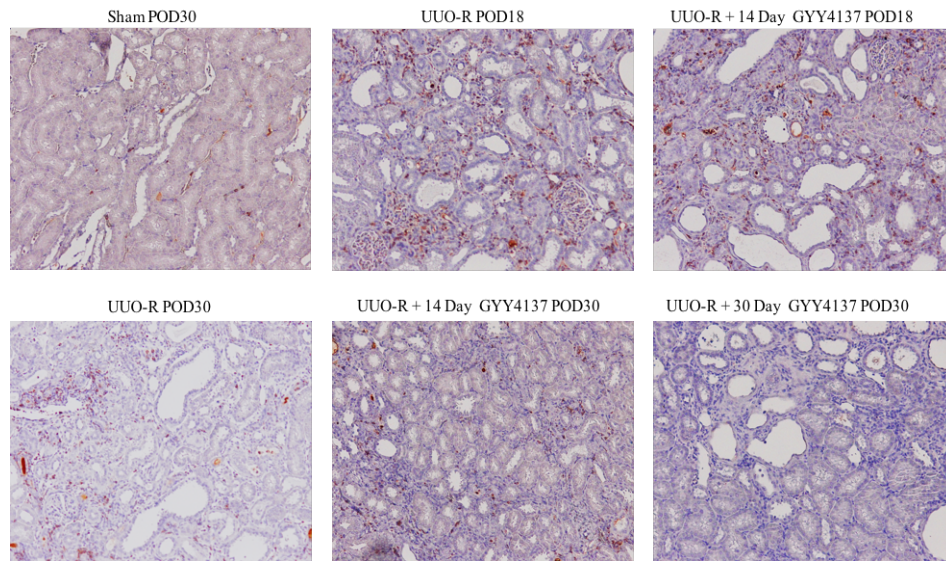


**Figure 9. Supplemental H<sub>2</sub>S reduces neutrophil infiltration following long-term UUO and relief of obstruction.** Immunohistochemistry staining of kidneys on POD 18 and 30 from Sham (n=5), UUO-R (n=10, 1mL PBS IP daily), UUO-R + 14 Day GYY4137 (n=11, 200  $\mu$ mol/kg GYY4137 in 1 mL PBS, IP daily POD 1-14), UUO-R + 30 Day GYY4137 (n=5, 200  $\mu$ mol/kg GYY4137 in 1 mL PBS, IP daily POD 1-30) rats using antibody against myeloperoxidase (MPO). A) Representative images of sections taken at 10x magnification. B) MPO-positive cells were quantified using ImageJ. Data represents median cell count of 5 randomly acquired images. Bar represents mean. \*  $p < 0.05$ , \*\*  $p < 0.01$  vs Sham POD30, †  $p < 0.05$  vs UUO-R POD30

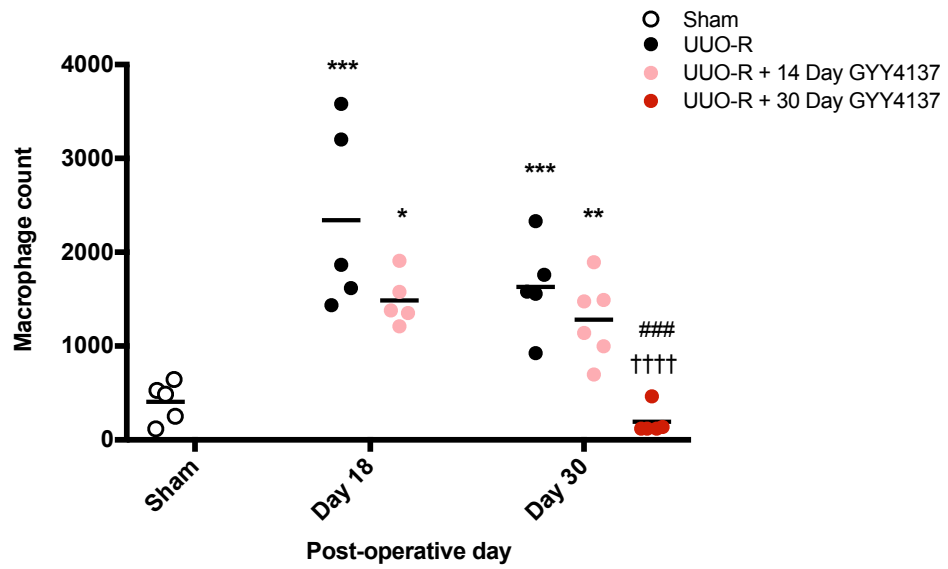
### 3.9 Supplemental H<sub>2</sub>S mediates macrophage infiltration

Kidney sections were immunohistochemically stained with antibodies against CD68 to determine the effects of GYY4137 on macrophage infiltration (Figure 10A). Compared to Sham, the level of macrophage infiltration in UUO-R and UUO-R + 14 Day GYY4137 animals were significantly higher on POD 18 and POD 30 ( $p < 0.0001$  and  $p < 0.05$  on POD 18,  $p < 0.001$  and  $p < 0.01$  on POD 30, respectively). While it was not statistically significant, there was a considerable decrease in macrophage infiltration in UUO-R + 14 Day GYY4137 when compared to UUO-R on POD 18 (Figure 10B). There was no difference in macrophage infiltration between Sham and UUO-R + 30 Day GYY4137 animals on POD 30. Interestingly, on POD 30, not only was the macrophage infiltration significantly lower in UUO-R + 30 Day GYY4137 when compared to UUO-R ( $p < 0.0001$ ), it was also significantly lower than UUO-R + 14 Day GYY4137 ( $p < 0.001$ , Figure 10B). To further elucidate the subtypes of infiltrating macrophages, kidney sections were immunofluorescently stained with antibodies against CD68 and CD206 (Figure 10C). M2 macrophages were deemed to be both CD68-positive and CD206-positive, and expressed as a percentage of total CD68-positive cells (Figure 10C). Interestingly, there was a significant increase in M2 macrophage infiltration in UUO-R + 14 Day GYY4137 group, but not UUO-R group, on POD 18 when compared to Sham ( $p < 0.05$ ). While not statistically significant, the infiltration of M2 macrophages was slightly higher in the UUO-R + 14 Day GYY4137 group when compared to UUO-R group on POD 18 (Figure 10D). The population of M2 macrophages in UUO-R, UUO-R + 14 Day GYY4137 and UUO-R + 30 Day GYY4137 was no different from Sham on POD 30 (Figure 10D).

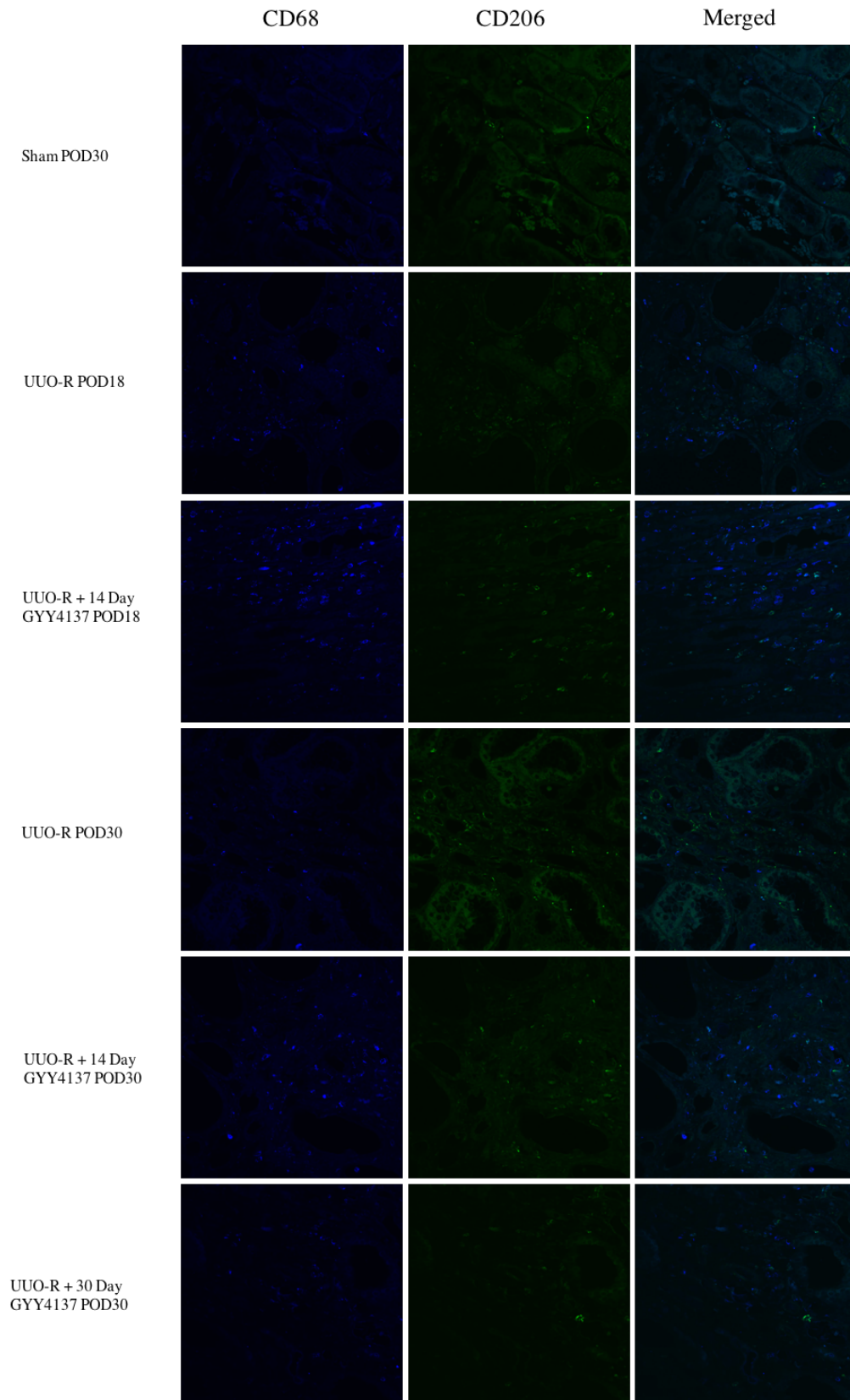
A)



B)



C)



D)

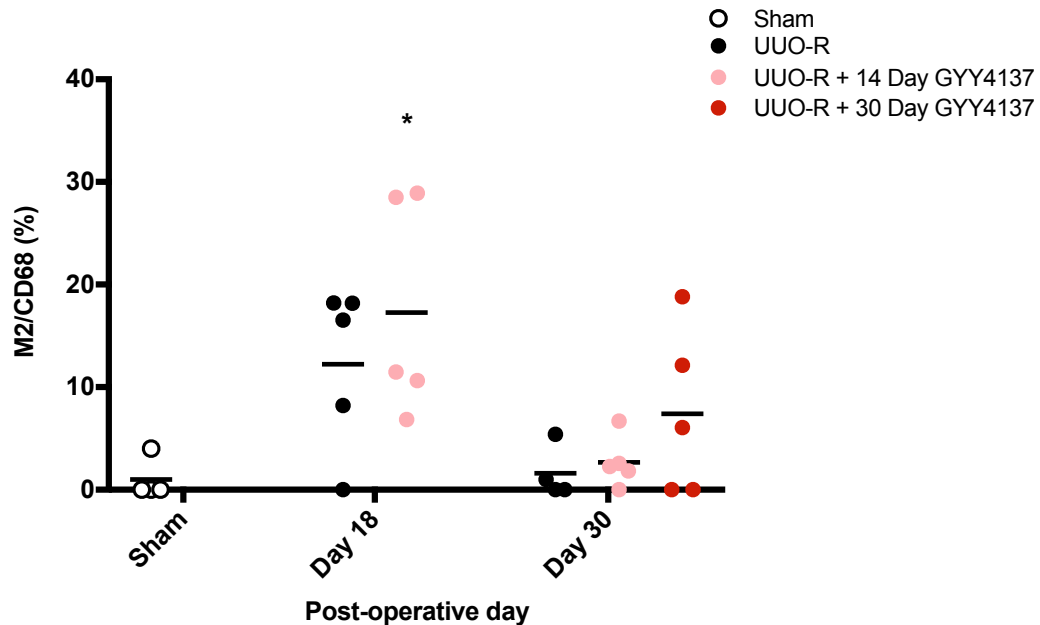


**Figure 10. GYY4137 mediates macrophage infiltration in urinary obstruction.**

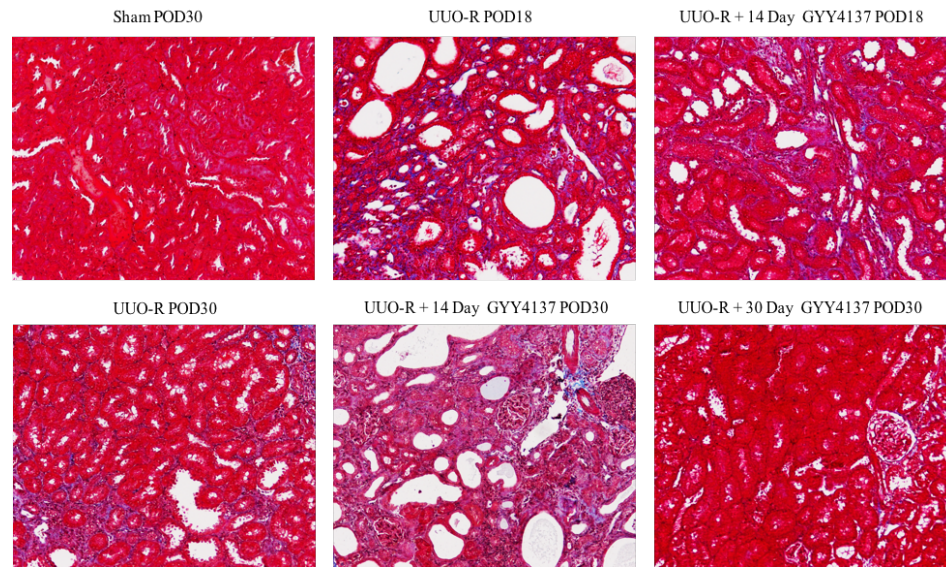
Kidney samples were obtained on POD 18 and 30 from Sham (n=5), UUO-R (n=10, 1mL PBS IP daily), UUO-R + 14 Day GYY4137 (n=11, 200  $\mu$ mol/kg GYY4137 in 1 mL PBS, IP daily POD 1-14), UUO-R + 30 Day GYY4137 (n=5, 200  $\mu$ mol/kg GYY4137 in 1 mL PBS, IP daily POD 1-30) rats. A) Representative images of sections stained with antibody against CD68 via IHC at 10x magnification. B) Positively stained cells were quantified using ImageJ. Data represents median cell count of 5 randomly acquired images at 10x magnification. Bar represents mean. C) Immunofluorescent staining of sections using antibodies against CD68 (blue) and CD206 (green). 5 images were acquired at random at 40x magnification. D) Using ImageJ to quantify positively-stained cells, CD68+/CD206+ cells (cyan) was normalized to CD68+ (blue). Data represents median percentage of M2 macrophage relative to total macrophage infiltrate. Bar represents mean. \* p<0.05, \*\*p<0.01, \*\*\*p<0.001 vs Sham POD30, ††††p<0.0001 vs UUO-R POD30, ####p<0.001 vs UUO-R + 14 Day GYY4137 POD 30.



### 3.10 Exogenous H<sub>2</sub>S ameliorates renal fibrosis following relief of prolonged UUO

Kidney sections were stained with Masson's trichrome to determine the level of renal fibrosis following decompression of long-term UUO (Figure 11A). On POD 18, UUO-R animals, but not UUO-R + 14 Day GYY4137 animals, exhibited significantly higher levels of fibrosis when compared to Sham ( $p < 0.05$ ). While not statistically significant, UUO-R + 14 Day GYY4137 animals had slightly lower levels of renal fibrosis when compared to UUO-R animals on POD 18 ( $p = 0.0732$ , Figure 11B). When compared to Sham, UUO-R, UUO-R + 14 Day GYY4137 and UUO-R + 30 Day GYY4137 animals all exhibited significantly higher levels of renal fibrosis on POD 30 ( $p < 0.001$ ,  $p < 0.05$ , and  $p < 0.05$ , respectively). Interestingly, both 14-day and 30-day treatment with GYY4137 significantly reduced renal fibrosis when compared to UUO-R animals on POD 30 ( $p < 0.05$ , Figure 11B).

A)



B)

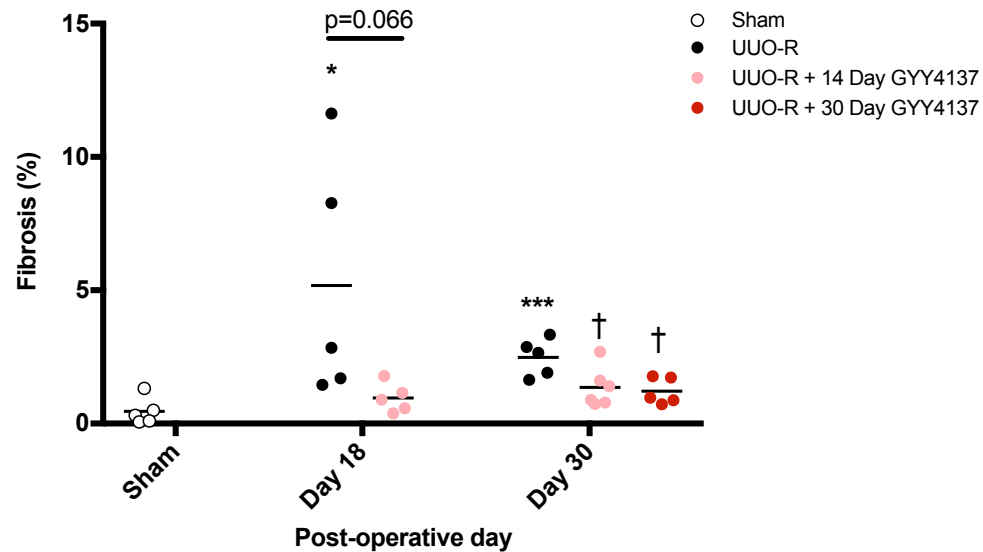


**Figure 11. H<sub>2</sub>S treatment mitigates renal fibrosis following prolonged UUO and decompression.** Kidneys were obtained on POD 18 and 30 from Sham (n=5), UUO-R (n=10, 1mL PBS IP daily), UUO-R + 14 Day GYY4137 (n=11, 200  $\mu$ mol/kg GYY4137 in 1 mL PBS, IP daily POD 1-14), UUO-R + 30 Day GYY4137 (n=5, 200  $\mu$ mol/kg GYY4137 in 1 mL PBS, IP daily POD 1-30) rats. A) Sections were stained with Masson's trichrome. Representative images of sections taken at 10x magnification. B) Fibrotic areas were quantified using ImageJ. Data represents median percentage of fibrosis of 5 randomly acquired images. Bar represents mean. \*  $p < 0.05$ , \*\*\* $p < 0.001$  vs Sham POD30, † $p < 0.05$  vs UUO-R POD30.

### 3.11 H<sub>2</sub>S attenuates the TGF- $\beta$ 1-mediated EMT pathway *in vitro*

To further evaluate the role of GYY4137 on fibrosis and elucidate potential mechanisms of action, rat kidney epithelial (NRK52E) cells were treated with 10 ng/mL TGF- $\beta$ 1 to induce EMT in the presence or absence of GYY137. Western blot analysis was completed to determine the expression of E-cadherin, vimentin, TGF- $\beta$ 1R2, Smad3, Smad7, and angiotensin II type 2 receptor (Figure 12).

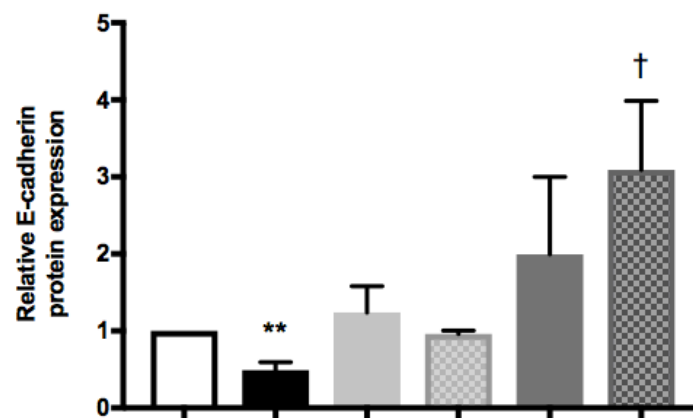
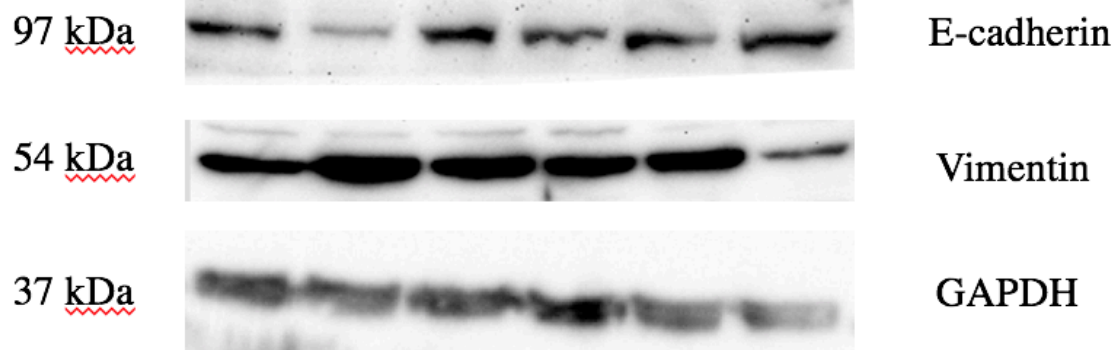
Both 10 and 50  $\mu$ M of GYY4137 alone had no effect on E-cadherin expression when compared to untreated cells. Interestingly, E-cadherin expression was significantly reduced upon treatment with 10 ng/mL TGF- $\beta$ 1 ( $p < 0.01$ ); however, the effect of TGF- $\beta$ 1 was slightly attenuated in the presence of 10  $\mu$ M GYY4137 and significantly abrogated in the presence of 50  $\mu$ M GYY4137 ( $p < 0.05$ , Figure 12A). The expression of vimentin in NRK52E cells remained unchanged relative to untreated cells in the presence of 10 ng/mL TGF- $\beta$ 1, 10  $\mu$ M GYY4137 and 50  $\mu$ M GYY4137. However, when compared to TGF- $\beta$ 1-treated cells, the expression of vimentin was slightly decreased in 10ng/mL TGF- $\beta$ 1 + 10  $\mu$ M GYY4137 cells, and significantly reduced in 10ng/mL TGF- $\beta$ 1 + 50  $\mu$ M GYY4137 cells ( $p < 0.05$ , Figure 12A).

Relative to untreated cells, Western blot analysis showed that the expression of Smad3 in 10 ng/mL TGF- $\beta$ 1, 10  $\mu$ M GYY4137, 50  $\mu$ M GYY4137, and 10 ng/mL TGF- $\beta$ 1 + 10  $\mu$ M GYY4137-treated cells remained unchanged (Figure 12B). However, when compared to 10 ng/mL TGF- $\beta$ 1-treated cells, expression of Smad3 was significantly reduced ( $p < 0.05$ ) upon additional treatment with 50  $\mu$ M GYY4137 (Figure 12B). Similarly, the expression of Smad7 in NRK52E cells remained unchanged in the presence of 10 ng/mL TGF- $\beta$ 1, 10  $\mu$ M GYY4137, and 50  $\mu$ M GYY4137 relative to untreated cells. However, when compared to TGF- $\beta$ 1-treated cells, expression of Smad7 was

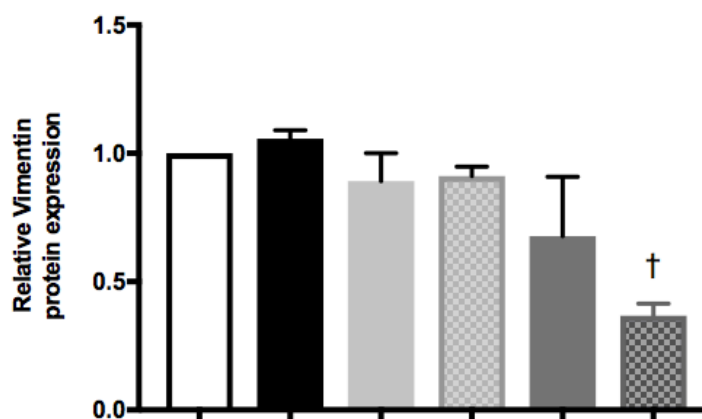
slightly increased in 10 ng/mL TGF- $\beta$ 1 + 10  $\mu$ M GYY4137-treated cells and significantly increased in 10 ng/mL TGF- $\beta$ 1 + 50  $\mu$ M GYY4137-treated cells ( $p < 0.05$ , Figure 12B).

In the presence of 10 or 50  $\mu$ M GYY4137 only, the expression of TGF- $\beta$ 1R2 in NRK52E cells remained unchanged relative to untreated cells. However, stimulating NRK52E cells with 10 ng/mL TGF- $\beta$ 1 significantly increased the expression of TGF- $\beta$ 1R2 ( $p < 0.05$ ) when compared to untreated cells. While this effect was not attenuated when 10  $\mu$ M GYY4137 was added, the effect of TGF- $\beta$ 1 on TGF- $\beta$ 1R2 expression was significantly reduced upon treatment with 50  $\mu$ M GYY4137 ( $p < 0.05$ , Figure 12C). While not statistically different, the expression of AT2R was slightly decreased in the presence of 10 ng/mL TGF- $\beta$ 1 when compared to untreated cells. Treatment with 10  $\mu$ M GYY4137 and 50  $\mu$ M GYY4137 had no effect on AT2R expression when compared to untreated cells. When compared to 10 ng/mL TGF- $\beta$ 1-treated cells, the expression of AT2R in 10 ng/mL TGF- $\beta$ 1 + 10  $\mu$ M GYY4137 remained unchanged, however, a slight increase in AT2R expression was observed in 10 ng/mL TGF- $\beta$ 1 + 50  $\mu$ M GYY4137-treated cells, though it was not statistically significant (Figure 12C).

A)

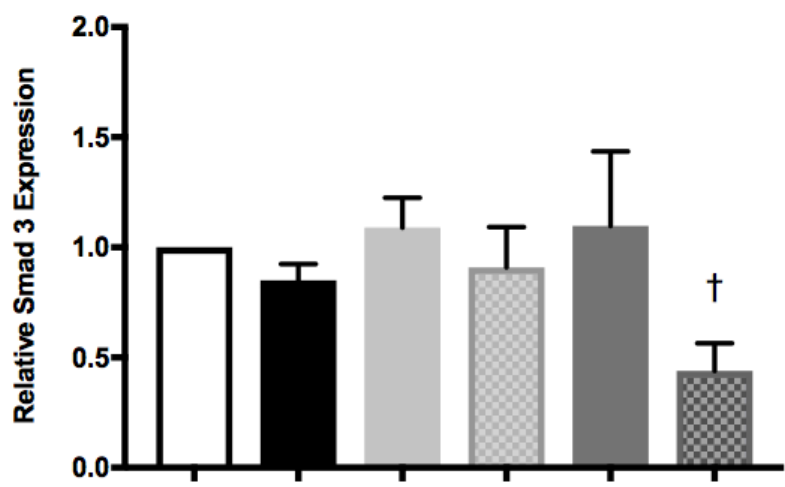
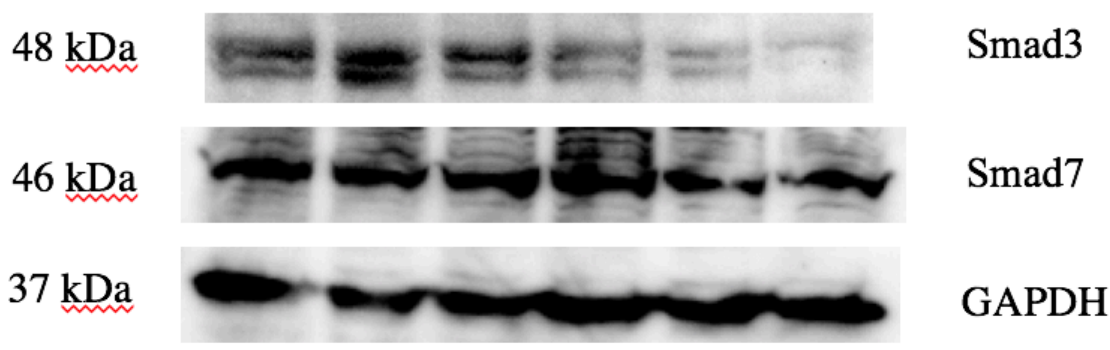


10ng/mL TGF-β1	-	+	-	-	+	+
10 μM GYY4137	-	-	+	-	+	-
50 μM GYY4137	-	-	-	+	-	+

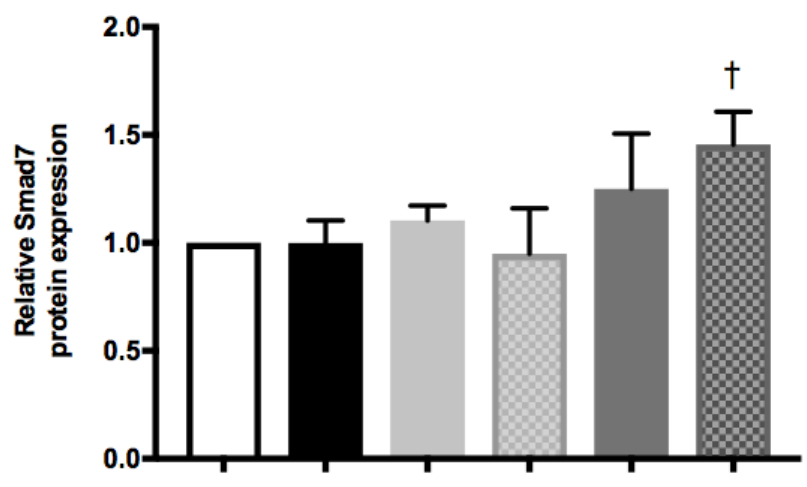


10ng/mL TGF-β1	-	+	-	-	+	+
10 μM GYY4137	-	-	+	-	+	-
50 μM GYY4137	-	-	-	+	-	+

B)



10ng/mL TGF-β1	-	+	-	-	+	+
10 μM GYY4137	-	-	+	-	+	-
50 μM GYY4137	-	-	-	+	-	+



10ng/mL TGF-β1	-	+	-	-	+	+
10 μM GYY4137	-	-	+	-	+	-
50 μM GYY4137	-	-	-	+	-	+

C)

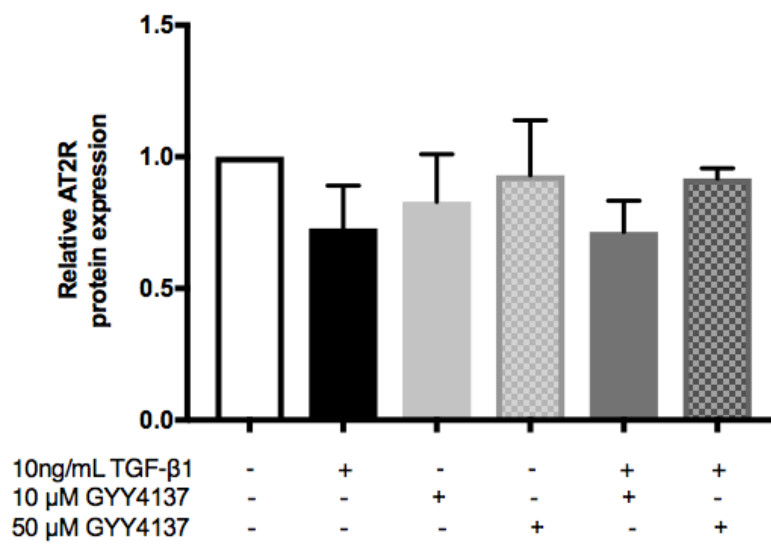
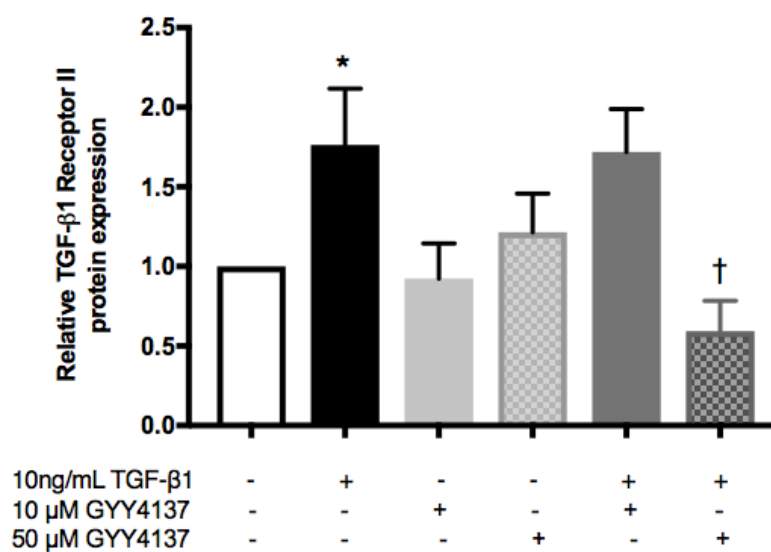
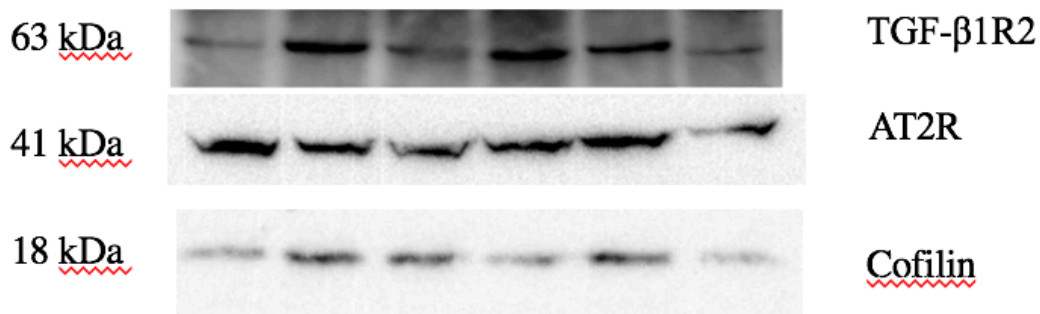


**Figure 12. H<sub>2</sub>S mitigates the TGF- $\beta$ 1-induced epithelial-mesenchymal transition in NRK52E cells.** NRK52E cells were subjected to treatment with 10 ng/mL TGF- $\beta$ 1, 10  $\mu$ M GYY4137, 50  $\mu$ M GYY4137, 10 ng/mL TGF- $\beta$ 1 + 10  $\mu$ M GYY4137, 10 ng/mL TGF- $\beta$ 1 + 50  $\mu$ M GYY4137, or left untreated in serum-free media (FBS-) for 48 hours. Total protein was isolated and assess for expression of A) E-cadherin and vimentin, B) Smad3 and Smad7, and C) TGF- $\beta$ 1R2 and AT2R, as well as housekeeping genes GAPDH and cofilin by means of western blot analysis. Expression levels were quantified by densitometry using ImageJ software and normalized to housekeeping genes. Data represents protein expression relative to FBS-. Data are mean  $\pm$  SEM, n=3. \*p<0.05 vs FBS-, †p<0.05 vs 10 ng/mL TGF- $\beta$ 1



## Chapter 4

### 4 Discussion

#### 4.1 Summary of study

If prolonged, urinary obstruction can lead to disruption of hemodynamics and renal function, such as reduced renal blood flow and defective sodium/potassium ATPase pumps (Klahr 2000). In addition, the accumulation of ROS can cause tubular injury and cell death and potentiate tissue inflammation (Ucero et al. 2014). These infiltrating leukocytes express a large variety of cytokines, including TGF- $\beta$ 1, a critical player in the induction of tissue fibrosis. Through the well-characterized Smad-dependent EMT pathway, TGF- $\beta$ 1 stimulates fibrosis and increases collagen deposition in the tubulointerstitial space (Ucero et al. 2014). It is important to note that, while obstructions can be surgically removed, renal function may not fully recovery as it is dependent on the duration and severity of the obstruction (Vaughan JR. & Gillenwater 1971). Although current pharmacological treatments may mediate pain associated with urinary obstruction, they do not attenuate the accumulation of renal injury. As a result, permanent renal dysfunction may occur following decompression. Thus, pre-emptively limiting renal injury during the course of obstruction may potentially improve renal function following relief of urinary obstruction (Chevalier et al. 1999).

Evidence suggests that H<sub>2</sub>S, an endogenously produced gaseous molecule, can cause vasodilation, scavenge ROS, and ameliorate apoptosis, inflammation, EMT and fibrosis in various models of tissue injury (Wang 2002; Lobb et al. 2014; Jung et al. 2013; Song et al. 2014). We have recently shown that GYY4137, a slow-releasing H<sub>2</sub>S donor, can mitigate renal injury and fibrosis in long-term UUO (Lin et al. 2016). Taken together, these studies suggest that H<sub>2</sub>S may be a potential therapy against renal injury associated with UUO. However, the UUO model is limited in its ability to provide accurate functional data. Therefore, in this study, we employed a rat model of UUO-R (a reversible UUO model) to evaluate the effects of H<sub>2</sub>S donor GYY4137 on renal function

and renal injury following relief of prolonged urinary obstruction. Furthermore, using an *in vitro* model of EMT, we elucidated potential mechanisms of action. We found that daily administration of GYY4137 improved renal function and mitigated renal injury. Our data suggests that GYY4137 may attenuate fibrosis by modulating the TGF- $\beta$ 1-mediated, Smad-dependent EMT pathway.

## 4.2 H<sub>2</sub>S from GYY4137 localizes to the kidney

NaHS and Na<sub>2</sub>S are two of the most commonly-used exogenous H<sub>2</sub>S molecules in the literature. These sulfide salts readily deliver H<sub>2</sub>S in solution, and due to their widespread availability, are easily accessible. However, sulfide salts release supra-physiological amounts of H<sub>2</sub>S rapidly, and thus fail to mimic the physiological production of H<sub>2</sub>S. In addition, the uncontrolled release of H<sub>2</sub>S can lead to off-target effects (Rose et al. 2015). To overcome this shortcoming, there has been a recent burst in the development of organic molecules that slowly release H<sub>2</sub>S to better mimic endogenous H<sub>2</sub>S production.

GYY4137 is a slow-releasing H<sub>2</sub>S donor that has been shown to exhibit vasodilatory, antihypertensive, and anti-inflammatory effects (Li et al. 2008; Li et al. 2013). Previous studies have shown that, unlike NaHS, intravenous and intraperitoneal injections of GYY4137 resulted in a sustained increase of plasma H<sub>2</sub>S, suggesting that GYY4137 releases H<sub>2</sub>S slowly over time and causes a systemic elevation in H<sub>2</sub>S (Li et al. 2008). However, we sought to determine whether intraperitoneal injection of GYY4137 causes H<sub>2</sub>S to reach the kidneys. As such, we obstructed the ureter for 3 days, with or without daily IP injections of GYY4137, then collected the kidney directly from the obstructed ureter. Using MeRho-Az, a fluorescent H<sub>2</sub>S probe (Hammers et al. 2015), we found increased levels of urinary H<sub>2</sub>S in animals treated with GYY4137 (Figure 2). Taken together, these results suggest that the H<sub>2</sub>S released from GYY4137 localizes to the kidneys.

### 4.3 H<sub>2</sub>S accelerates the recovery of renal function

Prolonged complete UUO inflicts severe damage to the obstructed kidney, leading to irreversible renal injury and dysfunction (Ucero et al. 2014). After 14 days of complete UUO, two animals in the UUO-R group died of renal failure following decompression, however, supplemental H<sub>2</sub>S led to 100% survival rate post-decompression (Figure 3). This suggests that H<sub>2</sub>S treatment could potentially be used as a treatment in UUO to minimize renal injury and improve functional recovery.

Serum creatinine and serum cystatin C are commonly-used indicators of renal function. During the obstructive phase, serum creatinine was significantly higher in UUO-R animals on POD 3 and 7, but with time, recovered back to Sham levels on POD 10. Liu et al. have observed a similar trend in a porcine model of UUO. When compared to pre-obstructive values, serum creatinine collected from bilateral renal veins and precaval veins were all significantly higher in UUO pigs (Liu et al. 2016). This suggests that UUO not only affects renal function of the obstructed kidney, but it has a moderate impact the contralateral kidney as well, thus resulting in a systemic elevation of serum creatinine.

Following relief of obstruction, we also removed the contralateral kidney such that the rat is dependent solely on the previously obstructed kidney. As expected, serum creatinine of experimental groups was elevated on POD 17, and despite a moderate decline over time, remained elevated on all post-operative days following decompression (Figure 4A). Our serum cystatin C data mirrored this trend; we observed an increase in serum cystatin C in all experimental groups on POD 18 when compared to Sham. By POD 30, a drastic decrease in serum cystatin C is observed, however it remains considerably higher than Sham (Figure 4B). This implies that prolonged urinary obstruction inflicts severe renal injury, and that recovery of renal function may not be complete despite surgical decompression (Vaughan JR. & Gillenwater 1971; Chaabane et al. 2013). However, we

observed a considerable decrease in serum creatinine on POD 17 in our 30-day GYY4137 treatment group, when compared to UUO-R (Figure 4A). This trend was also observed in our cystatin C data. While all experimental groups exhibited significantly higher serum cystatin C when compared to Sham on POD 18, GYY4137 treatment resulted in a moderate decrease in serum cystatin C. While it was not statistically significant, this reduction in serum creatinine and cystatin C could have important clinical and biological implications, and may suggest that GYY4137 treatment can lead to an earlier recovery of renal function following the relief of urinary obstruction. H<sub>2</sub>S could play a role in accelerating the recovery of renal function, as previously also demonstrated in IRI and transplant studies (Lobb et al. 2012).

Post-obstructive diuresis is characterized by heightened excretion of water and electrolytes following the relief of urinary obstruction. In rats, this can be observed following bilateral ureteral obstruction or UUO with contralateral nephrectomy (Harris & Yarger 1975). Post-obstructive diuresis can be caused by improper tubular reabsorption, and as a result, a robust increase in FENa is typically observed following decompression (Harris & Yarger 1975). In present study, we observed a drastic increase in FENa in all experimental groups 3 days following relief of obstruction and contralateral nephrectomy when compared to sham-operated animals (Figure 5). However, this was markedly ameliorated upon daily treatment of GYY4137, and interestingly, continuous administration of GYY4137 following relief of obstruction resulted in a more evident reduction of FENa (Figure 5). It is well-established that Na<sup>+</sup>/K<sup>+</sup> ATPases are critical in the maintenance of tubular sodium reabsorption and disruption of these channels can lead to increased FENa (Li et al. 2003). Previous studies have shown that the downregulation of tubular Na<sup>+</sup>/K<sup>+</sup> ATPases typically seen in UUO is likely a result of oxidative stress, which was mitigated upon administration of anti-oxidant apocynin (Liu et al. 2015). It is likely that H<sub>2</sub>S donor GYY4137 was protective in the same manner; due to its anti-oxidant properties, it was able to mitigate the downregulation of Na<sup>+</sup>/K<sup>+</sup> ATPases channels during UUO (Cao & Bian 2016). While all groups exhibit a slight recovery of

post-obstructive FENa by POD 30, it is important to note that GYY4137 accelerated the reduction of FENa after decompression.

Taken together, our data suggest that recovery of renal function following prolonged UUO was not complete despite surgical decompression. However, treatment with H<sub>2</sub>S donor GYY4137 during both the obstructive and recovery phase was beneficial as it accelerated the recovery of renal function as exemplified by the reduction of serum creatinine, serum cystatin C and FENa.

#### 4.4 Daily administration of H<sub>2</sub>S mitigates renal injury

To investigate the effect H<sub>2</sub>S on renal injury associated with UUO and decompression, we evaluated 24-hour total urine protein excretion as proteinuria is a well-established marker of renal injury. In the obstructive phase, 24-hour total urinary protein excretion remained the same across all experimental groups (Figure 6), likely due to the compensatory action of the contralateral kidney. However, following relief of obstruction and contralateral nephrectomy, we observed a significant increase in proteinuria in UUO-R group when compared to Sham. This was slightly mitigated upon treatment with GYY4137 during the obstructive phase (Figure 6). Proteinuria can be a sign of hypertensive injury (Helal et al. 2012; Lin et al. 2016). As previous studies have demonstrated that ACE inhibitors and angiotensin II type 1 receptor (AT1R) antagonists can reduce tissue damage and proteinuria (Suzuki et al. 2007), this suggests that the vasodilatory effects of H<sub>2</sub>S could play a role in mediating proteinuria and highlights its ability to regulate renal pressure (Lobb et al. 2014; Lin et al. 2016). We previously demonstrated a downregulation of AT1R expression following H<sub>2</sub>S treatment in UUO (Lin et al. 2016), which suggests that H<sub>2</sub>S does play an inhibitory role in the RAS. It is interesting to note that Ang II, a key player in regulating blood pressure, binds to both AT1R and angiotensin II type 2 receptors (AT2R). However, activation of AT2R counteracts the well-established effects of AT1R. In fact, AT2R has been shown to

exhibit vasodilatory, anti-inflammatory, anti-fibrotic, and anti-oxidative effects. In the renal system, AT2R has been shown to mediate renal blood flow and hypertensive renal disease (Chow & Allen 2016). Suzuki et al. further explored the effect of AT1R and AT2R activation in renal injury by examining their role on proteinuria. They discovered that the administration of AT1R antagonist ameliorated proteinuria, while treatment with AT2R agonist enhanced the expression of glomerular barrier proteins and led to decrease proteinuria (Suzuki et al. 2007). Furthermore, studies have shown the importance of NO in mediating AT2R expression and its corresponding vasodilatory effects (Chow & Allen 2016). As H<sub>2</sub>S share a multitude of properties, particularly vasodilation, with its gasotransmitter family member NO, it is possible that administration of H<sub>2</sub>S may have ameliorated proteinuria associated with urinary obstruction in a similar fashion. Further studies are required to determine the exact relationship and mechanism of action between H<sub>2</sub>S and AT2R.

Proteinuria can also occur due to hyperfiltration, which is often a result of nephron loss and reduction of renal cell mass (Helal et al. 2012). As H<sub>2</sub>S has been shown to increase tubular regeneration, it is possible that daily supplementation with H<sub>2</sub>S mitigated proteinuria by preserving renal architecture (Han et al. 2015; Lobb et al. 2015), thus diminishing hyperfiltration. This mirrors our histopathological data (Figure 6), where we demonstrate the ability of H<sub>2</sub>S to rescue cortical loss associated with UUO.

## 4.5 H<sub>2</sub>S mitigates the histopathological markers of renal injury following the relief of urinary obstruction

Significant cortical loss was observed in UUO-R and UUO-R + 14 Day GYY4137 groups on POD 18 and POD 30 when compared to Sham, however, we did not detect a difference in cortical thickness between UUO-R and UUO-R + 14 Day GYY4137 animal (Figure 7). The loss of renal cortex could be attributed to tissue atrophy and loss glomerular volume (Chaabane et al. 2013), which corresponds with the loss of renal function observed. Although we previously demonstrated that GYY4137 treatment helped to preserve renal architecture in UUO, this discrepancy may be due to the difference in injury model. Our previous study employed a 30-day obstruction model, which is much more severe than our current 14-day obstruction model; thus, the observed injury of UUO and protective effects of GYY4137 were more distinct (Lin et al. 2016). It is possible that we were not able to detect the subtler effects of GYY4137 in our present study. Interestingly, GYY4137 treatment both during obstruction and following decompression lead to a significant reduction in cortical loss when compared to UUO-R group on POD 30 (Figure 7). Previous studies have shown that H<sub>2</sub>S treatment lead to increased tubular proliferation and regeneration in ischemia-reperfusion injury by regulating cellular proliferation genes and maintaining blood flow (Han et al. 2015; Lobb et al. 2015). Taken together, this suggests that H<sub>2</sub>S can protect the kidney from cortical loss during prolonged UUO and treatment with H<sub>2</sub>S post-obstruction aids in recovery by accelerating tubular proliferation. These observed effects are likely attributed to the well-established ability of H<sub>2</sub>S to regulate blood flow (Xia et al. 2006).

Using TUNEL staining, we evaluated the effects of H<sub>2</sub>S on renal apoptosis 4 and 16 days post-decompression of 14-day obstruction. Unlike our previous 30-day UUO model, we were able to detect changes in renal apoptosis. Previous studies have shown that levels of apoptosis are elevated after 4 to 15 days of obstruction. However, a decline in apoptosis is observed after more than 15 days of obstruction as the kidney starts to exhibit more chronic injury phenotype (Truong et al. 1996; Lin et al. 2016). This suggests that apoptosis is an acute marker of renal injury and our previous 30-day obstruction model

resulted in a chronic injury phenotype. In present study, both UUO-R and UUO-R + 14 Day GYY4137 groups exhibited remarkable increase in renal apoptosis on POD 18 when compared to Sham. Although it was not statistically significant, treatment with GYY4137 throughout the course of obstruction slightly reduced renal apoptosis when compared to UUO-R animals. Apoptosis continues to be elevated in UUO-R and UUO-R + 14 Day GYY4137 groups on POD 30, however, continuous treatment with GYY4137 following the relief of obstruction mitigated renal apoptosis (Figure 8). This is likely due to the well-established anti-apoptotic effects of H<sub>2</sub>S and its ability to scavenge the ROS that accumulated from UUO (Szabó 2007; Koning et al. 2015).

To assess the effects of GYY4137 on inflammation, we quantified neutrophil and macrophage infiltration via IHC staining. As expected, a significant increase in neutrophil infiltration was observed in UUO-R and UUO-R + 14 Day GYY4137 animals on POD 18 and 30. Similar to our previous study, administration of H<sub>2</sub>S during the course of obstruction slightly reduced neutrophil infiltration on POD 18 when compared to UUO-R group (Lin et al. 2016). Interestingly, we observed a significant reduction in neutrophil infiltration in animals that continued to receive H<sub>2</sub>S treatment following decompression when compared to untreated animals and animals that received H<sub>2</sub>S treatment during the obstruction phase alone (Figure 9). Similarly, there was a significant increase in macrophage infiltration on POD 18 in both UUO-R and UUO-R + 14 Day GYY4137 groups on POD 18, however, the administration of GYY4137 led to a slight reduction in inflammation. We also observed a significant reduction in macrophage infiltration in animals that were given GYY4137 post-obstruction (Figure 9B). This is likely attributed to the well-established abilities of H<sub>2</sub>S to decrease leukocyte adhesion to vascular endothelial cells, inhibit the secretion of pro-inflammatory cytokines and stimulate the production of anti-inflammatory cytokines (Li et al. 2013; Szabó 2007).

The microenvironment of the kidney may alter macrophage activation and polarize macrophages towards M1 or M2 phenotypes. Classically activated (M1) macrophages



produce cytokines that induce inflammation and apoptosis, while alternatively activated (M2) macrophages secrete anti-inflammatory cytokines and contribute to tissue repair and regeneration (Kluth et al. 2004). We sought to distinguish the population of macrophages in renal tissue and evaluate the effects of H<sub>2</sub>S on macrophage polarization. Through immunofluorescent staining with macrophage marker CD68 and M2 marker CD206, we observed a significant increase in relative M2 population in UUO-R + 14 Day GYY4137 groups on POD 18 when compared to Sham, and a moderate increase when compared to UUO-R group (Figure 10D). This was expected, as studies have also observed an increase in relative M2 population following H<sub>2</sub>S supplementation in myocardial infarction and a corresponding recovery of cardiac function (Miao et al. 2016). Taken together, our data suggest that H<sub>2</sub>S helps to resolve inflammation by reducing total neutrophil and macrophage infiltration (Figures 9B and 10B), however, the increase in proportion of M2 macrophages implies that H<sub>2</sub>S either drives macrophages towards the M2 phenotype or depletes the relative proportion of pro-inflammatory M1 macrophages. It is possible that the reparative and anti-inflammatory properties of M2 macrophages may have also contributed to an earlier recovery of renal function following decompression (Miao et al. 2016).

Tubulointerstitial fibrosis is a hallmark of CKD and manifests as deposition of ECM into the interstitial space. After prolonged UUO, tubulointerstitial fibrosis is commonly observed and is a sign of severe renal injury (Eddy et al. 2012). To determine the effects of H<sub>2</sub>S following relief of UUO, we stained tissue sections with Masson's trichrome and observed a significant increase in renal fibrosis in UUO-R group on POD 18, and this remains elevated up until POD 30. GYY4137 treatment mitigated fibrosis on PODs 18 and 30 when compared to UUO-R group (Figure 11). Previous studies, including ours, observed a similar anti-fibrotic effect following administration of H<sub>2</sub>S, which suggests that H<sub>2</sub>S plays a protective role in mediating tissue fibrosis (Song et al. 2014; Lin et al. 2016; Jiang et al. 2013). Interestingly, our study demonstrated that H<sub>2</sub>S treatment mitigated renal fibrosis despite increasing the proportion of M2 macrophages. M2 macrophages, though anti-inflammatory and reparative, can secrete TGF- $\beta$ 1, which is a

known profibrotic cytokine (Meng et al. 2015). The role of M2 macrophages in fibrosis is heavily debated in the literature. While some studies have observed M2 macrophages in fibrotic regions and a corresponding reduction of fibrosis following depletion of M2 macrophages (Pan et al. 2015; Shen et al. 2014; Anders & Ryu 2011), others have observed a decrease in fibrosis despite a relative increase in M2 infiltration (Kushiyama et al. 2011). This suggests that the role of M2 macrophages in fibrotic injury requires further investigation. However, it is important to note that TGF- $\beta$ 1 is not exclusively profibrotic; it can also play an effective role in abating inflammation (Anders & Ryu 2011). Additionally, inflammation and epithelial healing are two of the first-line responses to injury, and tissue fibrosis only occurs if inflammation is unresolved and persistent (Meng et al. 2015; Anders & Ryu 2011). In this study, we observed a decline in total macrophage and neutrophil infiltration following H<sub>2</sub>S treatment (Figure 9B and 10B), but an increase in the relative proportion of M2 macrophages (Figure 10D). This suggests that overall inflammation was resolved upon H<sub>2</sub>S supplementation and therefore we did not observe an increase in renal fibrosis. Additionally, previous studies have shown that H<sub>2</sub>S treatment mitigates renal fibrosis associated with UUO by mitigating the TGF- $\beta$ 1-mediated EMT pathway (Song et al. 2014; Lin et al. 2016; Jiang et al. 2013). Therefore, it is possible that the overall anti-fibrotic properties of H<sub>2</sub>S is two-fold: it abrogates fibrosis directly by hindering the progression of EMT and indirectly by ameliorating tissue inflammation. To explore the direct anti-fibrotic effect of H<sub>2</sub>S further, we employed an *in vitro* model of EMT in rat kidney epithelial cells to elucidate the potential mechanisms of action.

It is particularly interesting that, despite a significant reduction in histopathological markers of renal injury following GYY4137 treatment, we were not able to detect a statistical difference in serum creatinine, cystatin C, FENa and urine protein between our UUO-R and our GYY4137-treated animals on POD 30. Our data implies that GYY4137 treatment may help accelerate the recovery of renal function. Though we were not able to detect a functional difference on POD 30, the reduction in histopathological markers of renal injury may have important implications on chronic renal function. In a

phenomenon known as “AKI to CKD”, studies have demonstrated that following AKI, patients may experience a moderate recovery of renal function, followed by a progressive loss of renal function over time (Cerdá et al. 2008). It appears that on POD 21 to POD 30, moderate recovery of renal function can be observed in all experimental groups. However, GYY4137 treatment resulted in a reduction in the histopathological markers of renal injury on POD 30; this could potentially be beneficial for long-term renal function. It is possible that GYY4137 can hinder the progression of AKI to CKD by mitigating inflammation and fibrosis in the kidney. However, future studies using chronic UUO-R models should be conducted to further explore the long-term progression of renal function following relief of urinary obstruction.

## 4.6 Elucidating the potential mechanisms of action

The increase in TGF- $\beta$ 1 leads to the induction of EMT in renal epithelial cells and ultimately results in tubulointerstitial fibrosis characteristic of CKD (Xu et al. 2009). Upon stimulation with TGF- $\beta$ 1, renal epithelial cells lose their epithelial properties, often characterized by the loss of epithelial marker E-cadherin, and become mesenchymal-like, as exemplified by the upregulation of vimentin. These cells can then migrate into the interstitial space and secrete ECM components. This pathway is heavily regulated by Smad proteins (it is stimulated by Smad3 and inhibited Smad7 (Ucero et al. 2014; Chevalier 2006)), and potentially indirectly abrogated by AT2R (Guo et al. 2016). We, along with others, have previously demonstrated that H<sub>2</sub>S treatment mitigates renal tubulointerstitial fibrosis associated with urinary obstruction (Lin et al. 2016; Jiang et al. 2013; Song et al. 2014). To elucidate the mechanism by which GYY4137 ameliorates fibrosis, we employed an *in vitro* model of EMT using rat kidney epithelial cells.

Upon TGF- $\beta$ 1 treatment, a downregulation of E-cadherin and a slight increase in expression of vimentin was observed. However, this was slightly abated upon treatment with 10  $\mu$ M of GYY4137 and significantly reduced with 50  $\mu$ M of GYY4137 (Figure

12A). This suggests that GYY4137 mitigates the TGF- $\beta$ 1-mediated EMT pathway, as previously shown (Jiang et al. 2013; Song et al. 2014), and it does so in a dose-dependent manner. Furthermore, NRK52E cells treated with 10  $\mu$ M and 50  $\mu$ M of GYY4137 alone did not express changes in expression of E-cadherin and vimentin (Figure 12A), which suggests that GYY4137 does not modulate the expression of EMT markers without TGF- $\beta$ 1 stimulation.

To further explore the Smad-dependent pathway of EMT, we investigated the expression of Smad3 and Smad7 in the presence of TGF- $\beta$ 1 and GYY4137. Unlike Smad3, Smad7 antagonizes the TGF- $\beta$  family signaling pathway as it can cause both Smad3 and TGF- $\beta$ 1 receptor 1 degradation (Yan et al. 2009). Smad7 is also heavily regulated: it is transcriptionally induced in the presence of TGF- $\beta$ 1, however, it itself is degraded in the process of degrading the TGF- $\beta$  receptor 1 (Yan et al. 2009). The constant turnover of Smad7 could have resulted in the seemingly lack of net change in Smad7 expression following TGF- $\beta$ 1 treatment (Figure 12B). Furthermore, we did not observe a change in total Smad3 expression following TGF- $\beta$ 1 treatment, which was expected as Smad3 is activated upon phosphorylation by TGF- $\beta$ 1 receptor (Wolf 2006) and the antibody used here only detects total Smad3 expression (Figure 12B). Previous studies have demonstrated a decrease in Smad3 phosphorylation following H<sub>2</sub>S treatment (Song et al. 2014; Jung et al. 2013), however we were not able to acquire a stable phosphorylated-Smad3 antibody. Interestingly, we observed an upregulation of Smad7 expression and a correlating downregulation of total Smad3 expression following treatment with TGF- $\beta$ 1 + 50  $\mu$ M GYY4137 (Figure 12B). This suggests that H<sub>2</sub>S may impede EMT progression by simulating Smad7 production, thereby reducing the number of Smad3s available for signal transduction. Our data may have elucidated a potentially novel mechanism by which H<sub>2</sub>S abrogates the progression of EMT, however further studies are required to elucidate the exact mechanism of action.

The AT2R can exhibit vasodilatory, anti-inflammatory, anti-fibrotic and renoprotective effects, and has been shown to counteract the classical vasoconstrictive effects of Ang II (Chow & Allen 2016). In addition, it can potentially mitigate fibrosis by decreasing the expression of TGF- $\beta$ 1R2 (Chow & Allen 2016; Guo et al. 2016). Interestingly, Guo et al. demonstrated that stimulation of AT2R inhibited the progression of TGF- $\beta$ 1-mediated EMT, which was heightened upon administration of NO donor SNAP and reversed upon treatment with NO synthase inhibitor L-NAME (Guo et al. 2016). As such, we sought to investigate the effects of H<sub>2</sub>S on AT2R expression. Although not statistically significant, treatment with TGF- $\beta$ 1 resulted in a subtle decrease in AT2R expression, which suggests that there is an antagonistic relationship between TGF- $\beta$ 1 and AT2R (Guo et al. 2016). Interestingly, this corresponded with a significant increase in TGF- $\beta$ 1R2 expression (Figure 12C), which was expected as this relationship was previously demonstrated by Guo et al (Guo et al. 2016). This effect was moderately reversed with the treatment with GYY4137 in a dose-dependent manner, returning the expression of AT2R back to baseline levels and significantly reducing the expression of TGF- $\beta$ 1R2 (Figure 12C). This suggests that, like NO, H<sub>2</sub>S may affect AT2R expression, and thus indirectly mitigate the progression of EMT. While subtle, this suggests a novel mechanism by which H<sub>2</sub>S can mediate the progression of EMT, however further studies, potentially involving receptor knockdowns, are required to fully characterize the effect of H<sub>2</sub>S on AT2R expression.

Taken together, we propose that H<sub>2</sub>S exhibits a two-fold modulation of the TGF- $\beta$ 1-mediated EMT pathway. It is likely that H<sub>2</sub>S may stimulate the production of inhibitory Smad7, thereby degrading the Smad3 proteins that are necessary for EMT signal transduction. Slightly upstream, it is also likely that H<sub>2</sub>S modulates EMT by subtly increasing the expression of AT2R, thereby abrogating the expression of TGF- $\beta$ 1R2 (Figure 13).

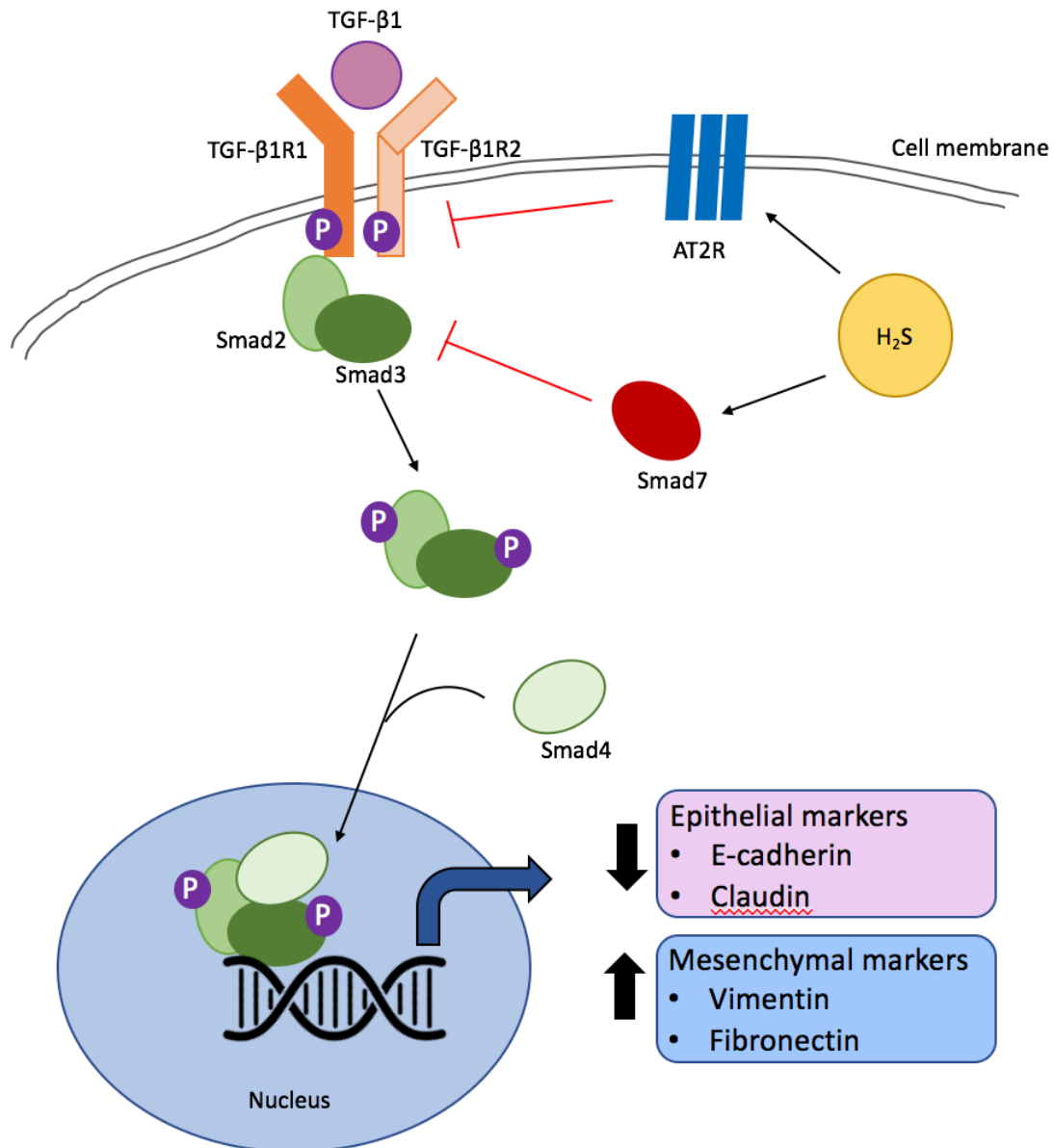


**Figure 13. Proposed mechanism of action of H<sub>2</sub>S in TGF-β1-mediated EMT pathway.** TGF-β1 binding to receptor phosphorylates Smad2 and Smad3, which then binds to Smad4 and translocate into the nucleus. In the nucleus, it acts as a transcription factor to increase the expression of mesenchymal markers, such as vimentin and fibronectin, and decrease the expression of epithelial characteristics. We propose that H<sub>2</sub>S acts by increasing AT2R, an upstream inhibitor of the TGF-β1 pathway, and Smad7, a negative regulator of EMT. This leads to the decreased expression of TGF-β1R2 and Smad3, and ultimately, the attenuation of fibrosis.

## 4.7 Conclusions and future implications

We demonstrate, for the first time, the effects of H<sub>2</sub>S on renal function following the relief of urinary obstruction by employing the UUO-R model. H<sub>2</sub>S supplementation during urinary obstruction and following decompression can accelerate the recovery of renal function, as demonstrated by reduction of serum creatinine and FENa. Furthermore, H<sub>2</sub>S can modulate urinary protein levels, which suggests that it is able to diminish renal injury due to hypertension and hyperfiltration. We propose that H<sub>2</sub>S mediates hypertension by acting on the AT<sub>2</sub>R, however, future studies should explore the exact mechanism and interaction. Additionally, we have demonstrated that H<sub>2</sub>S supplementation can help preserve renal architecture following UUO, likely due to its ability to increase tubular regeneration and proliferation. This could have also contributed to the reduction of proteinuria. Supplemental H<sub>2</sub>S also mitigated renal apoptosis, inflammation, and fibrosis associated with UUO. Interestingly, we found an increased proportion of M2 macrophages in renal tissue following H<sub>2</sub>S treatment, which suggests that H<sub>2</sub>S may have contributed to the resolution of inflammation by driving macrophages towards the reparative, anti-inflammatory M2 phenotype. However, the exact mechanism by which H<sub>2</sub>S regulates macrophage polarization is unknown. We recommend that future studies examine the relationship between the anti-inflammatory properties of H<sub>2</sub>S and its ability to drive macrophages towards the M2 subtype. As we observed a recovery in the histopathological markers of renal injury on POD 30, but did not observe a statistically significant difference in renal function following treatment with GYY4137, future studies should explore the long-term effects of GYY4137 on renal function following UUO-R. It is possible that GYY4137 treatment is able to impede the progression of AKI to CKD.

To elucidate potential mechanisms by which H<sub>2</sub>S ameliorates renal fibrosis, we employed an *in vitro* model of TGF- $\beta$ 1-mediated EMT in NRK 52E cells. We found that H<sub>2</sub>S supplementation attenuated the progression of EMT by upregulating inhibitory Smad7, which likely contributed to the degradation of signal transducer Smad3. Furthermore, H<sub>2</sub>S may potentially upregulate AT<sub>2</sub>R, an upstream regulator of the TGF- $\beta$ 1-mediated

EMT pathway, which ultimately led to the downregulation of TGF- $\beta$ 1R2, however, future studies should determine the exact mechanism by which H<sub>2</sub>S mediates AT2R expression.

Prolonged urinary obstruction can lead to irreversible renal injury and renal dysfunction. While various surgical treatments are available to remove the obstruction, recovery of renal function following decompression may not be complete. Currently, pharmacological interventions are typically used to mediate the severe flank pain associated with urinary obstruction, however, they do not mitigate the accumulation of renal injury. As the severity of renal injury is a strong determinant in the recovery of renal function, this suggests that reducing renal injury during urinary obstruction could lead to improved renal function following decompression. Our study has important clinical implications as we demonstrated that H<sub>2</sub>S treatment in urinary obstruction not only leads to a faster recovery of renal function, but it also mitigates renal injury and fibrosis. As such, H<sub>2</sub>S could be potentially be a therapeutic strategy in improving patient outcomes and renal function following urinary obstruction. As partial obstructions are more commonly seen in clinic, we suggest that future studies determine the effect of H<sub>2</sub>S on renal function following the relief of a partial obstruction. Furthermore, there has been a recent surge in the production of bioavailable H<sub>2</sub>S donors, such as ATB-346 (Wallace et al. 2017). To determine the role of H<sub>2</sub>S in renal recovery following urinary obstruction in a clinical setting, ATB-346 would be a potential candidate for future clinical trials involving patients with urinary obstruction.



## References

- Abe T, Fujino M, Yazawa K, Imamura R, Hatayama N, Kakuta Y, Tsutahara K, Okumi M, Ichimaru N, Kaimori JY, Isaka Y, Seki K, Takahara S, Li X-K, and N.N., 2017. High-pressure carbon monoxide preserves rat kidney grafts from apoptosis and inflammation. *Laboratory Investigation*, 0, pp.1–10.
- Anders, H.-J. & Ryu, M., 2011. Renal microenvironments and macrophage phenotypes determine progression or resolution of renal inflammation and fibrosis. *Kidney International*, 80(9), pp.915–925.
- Bauer, I. & Pannen, B.H.J., 2009. Bench-to-bedside review: Carbon monoxide--from mitochondrial poisoning to therapeutic use. *Critical care*, 13(4), pp.1–10.
- Cao, X. & Bian, J.-S., 2016. The Role of Hydrogen Sulfide in Renal System. *Frontiers in pharmacology*, 7(October), p.385.
- Cerdá, J. et al., 2008. Epidemiology of acute kidney injury. *Clinical Journal of the American Society of Nephrology*, 3(3), pp.881–886.
- Chaabane, W. et al., 2013. Renal functional decline and glomerulotubular injury are arrested but not restored by release of unilateral ureteral obstruction (UUO). *American Journal of Physiology: Renal Physiology*, 304(4), pp.F432-439.
- Chevalier, R.L., 2006. Pathogenesis of renal injury in obstructive uropathy. *Current opinion in pediatrics*, 18(2), pp.153–60.
- Chevalier, R.L. et al., 1999. Recovery following relief of unilateral ureteral obstruction in the neonatal rat. *Kidney International*, 55, pp.793–807.
- Chevalier, R.L., Forbes, M.S. & Thornhill, B.A., 2009. Ureteral obstruction as a model of renal interstitial fibrosis and obstructive nephropathy. *Kidney international*, 75(11), pp.1145–11452.

- Chow, B.S.M. & Allen, T.J., 2016. Angiotensin II type 2 receptor (AT2R) in renal and cardiovascular disease. *Clinical Science*, 130(15), pp.1307–1326.
- Eddy, A. a et al., 2012. Investigating mechanisms of chronic kidney disease in mouse models. *Pediatric Nephrology*, 27(8), pp.1233–1247.
- Gibbons, G.H., Pratt, R.E. & Dzau, V.J., 1992. Vascular Smooth Muscle Cell Hypertrophy vs . Hyperplasia Autocrine Transforming Growth Factor beta 1, Expression Determines Growth Response to Angiotensin II. *Journal of Clinical Investigation*, 90, pp.456–461.
- Gibbons, S.J. & Farrugia, G., 2004. The role of carbon monoxide in the gastrointestinal tract. *The Journal of physiology*, 556(Pt 2), pp.325–336.
- Guo, H.-L. et al., 2016. Angiotensin II Type 2 Receptor Decreases Transforming Growth Factor- $\beta$  Type II Receptor Expression and Function in Human Renal Proximal Tubule Cells. *PloS one*, 11(2), pp.e0148696, 1–15.
- Hammers, M.D. et al., 2015. A Bright Fluorescent Probe for H<sub>2</sub>S Enables Analyte-Responsive, 3D Imaging in Live Zebrafish Using Light Sheet Fluorescence Microscopy. *Journal of the American Chemical Society*, 137(32), pp.10216–10223.
- Han, S.J. et al., 2015. Hydrogen sulfide accelerates the recovery of kidney tubules after renal ischemia/reperfusion injury. *Nephrology Dialysis Transplantation*, 30(9), pp.1497–1506.
- Harris, R.H. & Yarger, W.E., 1975. The pathogenesis of post-obstructive diuresis. The role of circulating natriuretic and diuretic factors, including urea. *Journal of Clinical Investigation*, 56(4), pp.880–887.
- Helal, I. et al., 2012. Glomerular hyperfiltration: definitions, mechanisms and clinical implications. *Nature Reviews. Nephrology*, 8(5), pp.293–300.
- Iwano, M. & Neilson, E.G., 2004. Mechanisms of tubulointerstitial fibrosis. *Current opinion in nephrology and hypertension*, 13, pp.279–284.

- Jiang, D. et al., 2014. Exogenous hydrogen sulfide prevents kidney damage following unilateral ureteral obstruction. *Neurourology and Urodynamics*, 33, pp.538–543.
- Jiang, D. et al., 2013. Exogenous Hydrogen Sulfide Prevents Kidney Damage Following Unilateral Ureteral Obstruction. *Neurourology and Urodynamics*, 33(April), pp.538–543.
- Jung, K.-J. et al., 2013. Involvement of hydrogen sulfide and homocysteine transsulfuration pathway in the progression of kidney fibrosis after ureteral obstruction. *Biochimica et biophysica acta*, 1832(12), pp.1989–1997.
- Kaneto, H., Morrissey, J. & Klahr, S., 1993. Increased expression of TGF- $\beta$ 1 mRNA in the obstructed kidney of rats with unilateral ureteral ligation. *Kidney International*, 44(2), pp.313–321.
- Kerr JR, W.S., 1956. Effects of Complete Ureteral Obstruction in Dogs on Kidney Function. *American Journal of Physiology*, 184, pp.521–526.
- Klahr, S., 2000. Obstructive nephropathy. *Internal Medicine*, 39(5), pp.355–361.
- Kluth, D.C., Erwig, L.-P. & Rees, A.J., 2004. Multiple facets of macrophages in renal injury. *Kidney International*, 66, pp.542–557.
- Koning, A.M. et al., 2015. Hydrogen sulfide in renal physiology, disease and transplantation - The smell of renal protection. *Nitric oxide*, 46, pp.37–49.
- Kumar, S., Singh, R.K. & Bhardwaj, T.R., 2017. Therapeutic role of nitric oxide as emerging molecule. *Biomedicine & Pharmacotherapy*, 85, pp.182–201.
- Kushiyama, T. et al., 2011. Alteration in the phenotype of macrophages in the repair of renal interstitial fibrosis in mice. *Nephrology*, 16(5), pp.522–535.
- Lech, M. & Anders, H.-J., 2013. Macrophages and fibrosis: How resident and infiltrating mononuclear phagocytes orchestrate all phases of tissue injury and repair. *Biochimica et biophysica Acta*, 1832(7), pp.989–997.

- Lefer, A.M. & Lefer, D.J., 1999. Nitric oxide. II. Nitric oxide protects in intestinal inflammation. *The American Journal of Physiology*, 276(3 Pt 1), pp.G572-575.
- Li, C. et al., 2003. Altered expression of major renal Na transporters in rats with unilateral ureteral obstruction. *American Journal of Physiology. Renal Physiology*, 284(1), pp.F155-166.
- Li, L. et al., 2008. Characterization of a novel, water-soluble hydrogen sulfide-releasing molecule (GYY4137): new insights into the biology of hydrogen sulfide. *Circulation*, 117(18), pp.2351–2360.
- Li, L. et al., 2013. The complex effects of the slow-releasing hydrogen sulfide donor GYY4137 in a model of acute joint inflammation and in human cartilage cells. *Journal of cellular and molecular medicine*, 17(3), pp.365–376. Available at: <http://www.pubmedcentral.nih.gov/articlerender.fcgi?artid=3823018&tool=pmcentrez&rendertype=abstract> [Accessed August 27, 2015].
- Lin, S. et al., 2016. GYY4137, A Slow-Releasing Hydrogen Sulfide Donor, Ameliorates Renal Damage Associated with Chronic Obstructive Uropathy. *The Journal of Urology*, 196(December), pp.1778–1787.
- Liu, C. et al., 2015. Involvement of NOX in the regulation of renal tubular expression of Na/K-ATPase in acute unilateral ureteral obstruction rats. *Nephron*, 130(1), pp.66–76.
- Liu, Y. et al., 2016. A porcine model of relief of unilateral ureteral obstruction: study on self-repairing capability over multiple time points. *Molecular and Cellular Biochemistry*, 419(1–2), pp.115–123.
- Lobb, I. et al., 2015. Hydrogen sulfide treatment mitigates renal allograft ischemia reperfusion injury during cold storage and improves early transplant kidney function and survival following allogeneic renal transplantation. *The Journal of Urology*.
- Lobb, I. et al., 2014. Hydrogen sulphide and the kidney: Important roles in renal

- physiology and pathogenesis and treatment of kidney injury and disease. *Nitric Oxide: Biology and Chemistry/Official Journal of the Nitric Oxide Society*, 46(2015), pp.55–65.
- Lobb, I. et al., 2012. Supplemental hydrogen sulphide protects transplant kidney function and prolongs recipient survival after prolonged cold ischaemia-reperfusion injury by mitigating renal graft apoptosis and inflammation. *BJU international*, 110(11 Pt C), pp.E1187-1195.
- Manucha, W. et al., 2004. Losartan modulation on NOS isoforms and COX-2 expression in early renal fibrogenesis in unilateral obstruction. *Kidney International*, 65, pp.2091–2107.
- Meng, X.-M. et al., 2015. Macrophage Phenotype in Kidney Injury and Repair. *Kidney Diseases*, 1(2), pp.138–146.
- Miao, L. et al., 2016. Hydrogen Sulfide Mitigates Myocardial Infarction via Promotion of Mitochondrial Biogenesis-Dependent M2 Polarization of Macrophages. *Antioxidants & Redox Signaling*, 25(5), pp.268–281.
- Motterlini, R. & Foresti, R., 2013. Heme oxygenase-1 as a target for drug discovery. *Antioxidants & redox signaling*, 20(11), pp.1810–1826.
- Pan, B. et al., 2015. Regulation of renal fibrosis by macrophage polarization. *Cellular Physiology and Biochemistry*, 35(3), pp.1062–1069.
- Qian, Y. & Matson, J.B., 2016. Gasotransmitter delivery via self-assembling peptides: Treating diseases with natural signaling gases. *Advanced Drug Delivery Reviews*.
- Rose, P., Dymock, B.W. & Moore, P.K., 2015. *GY4137, a Novel Water-Soluble, H<sub>2</sub>S-Releasing Molecule*. 1st ed., Elsevier Inc.
- Roth, K.S. et al., 2002. Obstructive Uropathy: An Important Cause Chronic Renal Failure in Children. *Clinical Pediatrics*, 41, pp.309–314.

- Sakurai, H. et al., 1996. Activation of transcription factor NF- $\kappa$ B in experimental glomerulonephritis in rats. *Biochimica et Biophysica Acta*, 1316, pp.132–138.
- Samarakoon, R. et al., 2012. TGF- $\beta$ 1  $\rightarrow$  SMAD/p53/USF2  $\rightarrow$  PAI-1 transcriptional axis in ureteral obstruction-induced renal fibrosis. *Cell and tissue research*, 347(1), pp.117–128.
- Sharma, J.N., Al-Omran, A. & Parvathy, S.S., 2007. Role of nitric oxide in inflammatory diseases. *Inflammopharmacology*, 15(6), pp.252–259.
- Shen, B. et al., 2014. Macrophages Regulate Renal Fibrosis Through Modulating TGF $\beta$  Superfamily Signaling. *Inflammation*, 37(6), pp.2076–2084.
- Song, K. et al., 2015. Hydrogen Sulfide: A Therapeutic Candidate for Fibrotic Disease? *Oxidative medicine and cellular longevity*, 2015, p.Article ID 458720.
- Song, K. et al., 2014. Hydrogen sulfide inhibits the renal fibrosis of obstructive nephropathy. *Kidney international*, 85(6), pp.1318–1329.
- Sonke, E. et al., 2015. Inhibition of endogenous hydrogen sulfide production in clear-cell renal cell carcinoma cell lines and xenografts restricts their growth, survival and angiogenic potential. *Nitric Oxide: Biology and Chemistry*, 49, pp.26–39. Available at: <http://dx.doi.org/10.1016/j.niox.2015.06.001>.
- Spernat, D. & Kourambas, J., 2011. Urolithiasis – medical therapies. *BJU international*, 108, pp.9–13.
- Sun, D. et al., 2012. Effects of nitric oxide on renal interstitial fibrosis in rats with unilateral ureteral obstruction. *Life Sciences*, 90(23–24), pp.900–909.
- Suzuki, K. et al., 2007. Angiotensin II type 1 and type 2 receptors play opposite roles in regulating the barrier function of kidney glomerular capillary wall. *The American journal of pathology*, 170(6), pp.1841–1853.
- Szabó, C., 2007. Hydrogen sulphide and its therapeutic potential. *Nature reviews. Drug*

*discovery*, 6(11), pp.917–935.

- Tapmeier, T.T. et al., 2008. Reimplantation of the ureter after unilateral ureteral obstruction provides a model that allows functional evaluation. *Kidney international*, 73(7), pp.885–889.
- Truong, L.D. et al., 1996. Cell apoptosis and proliferation in experimental chronic obstructive uropathy. *Kidney international*, 50, pp.200–207.
- Truong, L.D. et al., 2001. Renal cell apoptosis in chronic obstructive uropathy : The roles of caspases. *Kidney international*, 60, pp.924–934.
- Ucero, A.C. et al., 2014. Unilateral ureteral obstruction: beyond obstruction. *International urology and nephrology*, 46(4), pp.765–776.
- Vaughan JR., E.D. & Gillenwater, J.Y., 1971. Recovery following complete chronic unilateral ureteral occlusion: functional, radiographic and pathologic alterations. *The Journal of Urology*, 106, pp.27–35.
- Wallace, J.L. et al., 2015. Gaseous mediators in resolution of inflammation. *Seminars in Immunology*, 27(3), pp.227–233.
- Wallace, J.L. et al., 2017. Hydrogen Sulfide-Releasing Therapeutics: Translation to the Clinic. *Antioxidants & Redox Signaling*.
- Wang, L. et al., 2008. Protective effects of low-dose carbon monoxide against renal fibrosis induced by unilateral ureteral obstruction. *American Journal of Physiology Renal:Physiology*, 294, pp.F508–F517.
- Wang, R., 2002. Two's company, three's a crowd: can H<sub>2</sub>S be the third endogenous gaseous transmitter? *FASEB journal: official publication of the Federation of American Societies for Experimental Biology*, 16(13), pp.1792–1798.
- Whiteman, M. et al., 2011. Emerging role of hydrogen sulfide in health and disease: critical appraisal of biomarkers and pharmacological tools. *Clinical science*,

121(11), pp.459–488.

- Wolf, G., 2006. Renal injury due to renin-angiotensin-aldosterone system activation of the transforming growth factor-beta pathway. *Kidney international*, 70(11), pp.1914–1919.
- Wu, A.K. et al., 2012. Relative renal function does not improve after relieving chronic renal obstruction. *BJU international*, 109(10), pp.1540–1544.
- Xia, M. et al., 2006. Production and Actions of Hydrogen Sulfide , a Novel Gaseous Bioactive Substance , in the Kidneys. *The Journal of Pharmacology and Experimental Therapeutics*, 329(3), pp.1056–1062.
- Xu, J., Lamouille, S. & Derynck, R., 2009. TGF-beta-induced epithelial to mesenchymal transition. *Cell research*, 19(2), pp.156–172.
- Xue, H. et al., 2013. H<sub>2</sub>S inhibits hyperglycemia-induced intrarenal renin-angiotensin system activation via attenuation of reactive oxygen species generation. *PloS one*, 8(9), p.e74366.
- Yamamoto, J. et al., 2013. Distribution of hydrogen sulfide (H<sub>2</sub>S)-producing enzymes and the roles of the H<sub>2</sub>S donor sodium hydrosulfide in diabetic nephropathy. *Clinical and experimental nephrology*, 17(1), pp.32–40.
- Yan, X., Liu, Z. & Chen, Y., 2009. Regulation of TGF-beta signaling by Smad7. *Acta biochimica et biophysica Sinica*, 41(4), pp.263–272.
- York, N.E., Borofsky, M.S. & Lingeman, J.E., 2015. Risks associated with drug treatments for kidney stones. *Expert opinion on drug safety*, 338, pp.1–13.



## Curriculum Vitae

**Name:** Shouzhe Lin

**Post-secondary Education and Degrees:** The University of Western Ontario  
London, Ontario, Canada  
2011-2015 BMSc

The University of Western Ontario  
London, Ontario, Canada  
2015-2017 MSc

**Honours and Awards:** Canadian Institutes of Health Research  
2016-2017

Lawson Internal Research Fund  
2015-2016

**Related Work Experience** Teaching Assistant  
The University of Western Ontario  
2015-2016

### Publications:

**Lin, S.**, Lian, D., Liu, W., Haig, A., Lobb, I., Hijazi, A., Whiteman, M., and Sener, A. 17-4642. Daily hydrogen sulfide therapy during prolonged ureteric obstruction enables early renal recovery following decompression. *The Journal of Urology*. 2017 April; 197 (4): S1-1376.

**Lin, S.**, and Sener, A. Is hydrogen sulfide, an endogenously derived gasotransmitter, a potential novel therapy for ureteric obstruction? *The Journal of Endourology*. 2017 April 10. Submitted.

Olvera-Posada, D., **Lin, S.**, Aboalsamh, G., Haig, A., Lobb, I., Grewal, J., Saha, M., and Sener, A. A novel approach to off-clamp partial nephrectomy demonstrates significant improvement in renal injury in an experimental porcine model. *Canadian Urological Association Journal*. 2016 November 22. Accepted.

**Lin, S.**, Visram, F., Liu, W., Haig, A., Jiang, J., Mok, A., Lian, D., Wood, M.E., Torregrossa, R., Whiteman, M., Lobb, I., and Sener, A. GYY4137, a slow-releasing hydrogen sulfide donor, ameliorates renal damage associated with chronic obstructive uropathy. *The Journal of Urology*. 2016 December 1; 196(6): 1778-1787.

**Lin, S.**, Visram, F., Lobb, I., Liu, W., Haig, A., Saha, M., Mok, A., Jiang, J., Lian, D., Wood, M.E., Whiteman, M., and Sener, A. P76 Supplemental hydrogen sulfide attenuates epithelial-mesenchymal transition and mitigates renal fibrosis associated with chronic obstructive uropathy. *4th International Conference on the Biology of Hydrogen Sulfide*. 2016 June 3. p.239-240.

Leigh, J., Shao, P., Saha, M., Lobb, I., Pasch, A., van Goor, H., Feelisch, M., Wang, R., **Lin, S.**, and Sener, A. P33 Deficiency in renal erythropoietin production is a result of impaired endogenous hydrogen sulfide production. *4th International Conference on the Biology of Hydrogen Sulfide*. 2016 June 3. p.142-143.

**Lin, S.**, Visram, F., Lobb, I., Liu, W., Haig, A., Saha, M., Mok, A., Jiang, J., Lian, D., Wood, M.E., Whiteman, M., and Sener, A. MP58-18 Exogenous hydrogen sulfide treatment reduces renal fibrosis associated with chronic ureteral obstruction by attenuating epithelial-mesenchymal transition. *The Journal of Urology*. 2016 May 10. 195(4): e783

D'Cruz, R., Plant, P., Correa, J., Pablo, L.A., **Lin, S.**, Chackowicz, J., Bain, J., and Batt, J. PDLIM7 is a novel target of the ubiquitin ligase Nedd4-1. *Biochemical Journal*. 2016 February 1. 473(3): 267-76.

**Lin, S.**, Visram F., Lobb, I., Mok, A., Jiang, J., Whiteman, M., Liu, W., Haig, A., Sener, A. Hydrogen sulfide ameliorates renal injury associated with chronic obstructive uropathy. *Canadian Urological Association Journal*. 9(9) S228, P91.